Enhanced NAPL Removal and Mixing with Engineered Chaotic Advection

Yufei Wang[1,2] **Daniel Fernàndez-Garcia**[1,2] **Guillem Sole-Mari**[3,1,2] **Paula Rodríguez-Escales**[1,2]

[1]Dept. of Civil and Environmental Engineering. Universitat Politècnica de Catalunya, Jordi Girona 1-3, 08034 Barcelona, Spain
[2]Associated Unit: Hydrogeology Group (UPC-CSIC)
[3]Earth and Environmental Sciences Area, Geochemistry Department, Lawrence Berkeley National Laboratory, 1 Cyclotron Rd, Berkeley, CA 94720, USA

Key Points:

- Chaotic advection enhances non-aqueous phase liquid removal and mixing in heterogeneous porous media while reducing uncertainty
- Removal efficiency increases to a maximum value when the injection pulse satisfies that the Kubo number is close to one
- The relative benefit of chaotic advection is substantially larger in conditions of unfavorable aquifer heterogeneity and connectivity

Corresponding author: Yufei Wang, yufei.wang@upc.edu

Abstract

Aquifer remediation with in situ soil washing techniques and enhanced oil removal typically involve the injection of liquid solutions into the geological formation to displace and mobilize non-aqueous phase liquids (NAPLs). The efficiency of these systems is oftentimes low because the displacing fluid bypasses large quantities of NAPL due to the inherent complexity of a heterogeneous natural system. Here, chaotic advection generated by a rotating periodic injection pulse is proposed as a method to enhance NAPL removal and mixing. To evaluate the method, we perform two-phase flow simulations in multiple realizations of random permeability fields with different correlation structures and connectivity between injection and extraction wells embedded in a five-spot pattern. Results show that chaotic advection can significantly improve removal efficiency and mixing depending on several controlling factors. Chaotic advection effects are more significant under unfavorable conditions, i.e., when injection and extraction wells are well-connected through preferential channels, permeabilities are highly heterogeneous, and/or the mobility ratio between the wetting and the non-wetting fluid is larger than one. Removal efficiency reaches its maximum value when the Kubo number is close to one, i.e., when the saturation front travels one range of the permeability field in an injection pulse. These effects can develop in just a few cycles. However, removal efficiency should undergo first an early stage with detrimental effects in order to maximize removal in the long term. Chaotic advection not only enhances NAPL removal and mixing, but also reduces the uncertainty, making the system more reliable and less dependent on heterogeneity.

1 Introduction

Non-aqueous phase liquid (NAPL) removal from complex geological formations is of great interest in aquifer remediation with in situ soil washing techniques [*Huling and Weaver*, 1991; *NRC*, 2005]. These techniques typically involve the injection of liquid solutions into the geological formation to displace and mobilize the target NAPL contaminant source (e.g., hydrocarbons, chlorinated solvents, mineral oil and other products from chemical industry) towards extraction wells [*Rao et al.*, 1997; *Martel et al.*, 2004; *Smalley et al.*, 2009; *Davies et al.*, 2014; *Jackson*, 2014; *Jin et al.*, 2017; *Welkenhuysen et al.*, 2017]. The injected fluid can be water or liquid solutions with cosolvents (e.g., hydroxypropyl-β-cyclodextrin), surfactants (e.g., sodium dihexyl sulfosuccinate) or polymers (e.g., partially hydrolyzed polyacrylamid), which are meant to improve sweeping and flushing by either reducing capillary trapping, increasing dissolution or reducing water mobility [*Falta et al.*, 1999; *Mccray and Brusseau*, 1999; *Dugan et al.*, 2003; *Yousefvand and Jafari*, 2015; *Javanbakht et al.*, 2017]. An early removal of NAPL can substantially eliminate the main contaminant source, improving the overall cleanup efficiency at later stages of the remediation process [*Huling and Weaver*, 1991; *Soga et al.*, 2004].

NAPL removal is more efficient in relatively homogeneous porous media and low mobility ratios [*Fayers and Hewett*, 1992; *Soga et al.*, 2004; *Smalley et al.*, 2009; *Stroo et al.*, 2012]. However, aquifer heterogeneity (the spatial distribution of permeability) often exhibits well-organized high permeability geological structures that concentrate the flow in the form of preferential channels [*de Marsily*, 1985; *Western et al.*, 2001; *Zheng and Gorelick*, 2003; *Knudby and Carrera*, 2005; *Le Borgne and Gouze*, 2008; *Fernàndez-Garcia et al.*, 2010; *Bianchi et al.*, 2011a; *Renard and Allard*, 2013a; *Essaid et al.*, 2015; *Nicolaides et al.*, 2015]. In a multiphase flow problem, these channels will cause the displacing fluid to bypass large quantities of the NAPL in place, resulting in a significant reduction of the sweeping efficiencies and the mixing between the wetting and the non-wetting phase [*Pruess and Tsang*, 1990; *Wan et al.*, 1996; *Glass et al.*, 1998; *Amundsen et al.*, 1999; *Bertels et al.*, 2001; *Rangel-German and Kovscek*, 2006; *Arshadi et al.*, 2017, 2018; *Kim et al.*, 2019]. The latter is crucial for chemical flooding with surfactants and cosolvents during the remediation of an aquifer contaminated with NAPL, as dissolution directly depends on the contact between

liquid phases. In the petroleum industry, channeling will cause huge losses in recovered oil and monetary income [*Craig et al.*, 1957; *Craig*, 1971; *Fayers and Hewett*, 1992; *Paez Yanez et al.*, 2007]. The injection of fluids in a multiphase system is also important for studying the sequestration of anthropogenic CO_2 in deep saline aquifers [e.g., *Bachu*, 2000; *Bolster et al.*, 2009; *Vilarrasa et al.*, 2010; *Saaltink et al.*, 2013], which constitutes an interesting alternative for reducing greenhouse gas emissions to the atmosphere.

Engineered chaotic advection has been demonstrated to be an efficient technique for enhancing in situ groundwater remediation technologies [e.g., *Zhang et al.*, 2009; *Mays and Neupauer*, 2012; *Trefry et al.*, 2012a; *Lester et al.*, 2013; *Neupauer et al.*, 2014; *Rodríguez-Escales et al.*, 2017; *Di Dato et al.*, 2018]. This technique generates chaotic advection by means of time-dependent water injection and extraction systems creating erratic transport paths that enhance mixing by folding and stretching the solute plume. Results in this area have shown that applying chaotic advection increases considerably the contact area between the contaminants and the injected treatment solutions during in situ remediation of contaminated groundwater, promoting the degradation of toxic compounds, including emerging organic contaminants [*Ottino*, 1990; *Ottino et al.*, 1994; *Bagtzoglou and Oates*, 2007; *Luo et al.*, 2008; *Rodríguez-Escales et al.*, 2017; *Libera et al.*, 2017]. There are different ways to generate chaotic advection in the subsoil. One of them is by using a rotated potential mixing flow (RPM). This form of chaotic advection can be generated by assemblies of several dipole injection/extraction wells operating in a plane with the same flow rate [*Metcalfe et al.*, 2006; *Lester et al.*, 2009, 2010; *Metcalfe et al.*, 2010; *Trefry et al.*, 2012b]. A necessary condition to generate chaos is the transient crossing of streamlines [*Lester et al.*, 2009], which is fulfilled with this technique. The simplest RPM-generating sequence consists in activating a dipole injection/extraction well for a certain time, then rotating the active dipole around the origin by an angle, and repeating periodically. However, the RPM flow is not the only way to generate chaotic advection in groundwater polluted sites. Many other kinds of well networks and stirring protocols have been proposed in literature with the objective of enhancing mixing of solutions in groundwater by inducing chaotic advection [e.g., *Bagtzoglou and Oates*, 2007; *Zhang et al.*, 2009; *Piscopo et al.*, 2013; *Neupauer et al.*, 2014].

Although some authors *Falta et al.* [1999] have already observed that altering the flow direction can improve NAPL remediation, there are no works aimed at evaluating the improvement of chaotic advection during in situ NAPL remediation. The study of this problem requires the simulation of a multiphase flow system, which at least should describe the movement of the wetting (injected fluid) and the non-wetting fluid (NAPL) through the porous medium [*Abriola and Pinder*, 1985; *Sleep and Sykes*, 1989; *Celia et al.*, 2015]. Under some simplifying conditions, the governing equation of saturation of immiscible fluids resembles the advection-dispersion equation (ADE) in porous media [*Sleep and Sykes*, 1993a,b; *Bolster et al.*, 2009]. However, the advective and the dispersive terms in the saturation equation are nonlinear functions of saturation, making impossible a direct extrapolation of the results obtained in solute transport.

Motivated by this similarity and the success of an engineered sequence of injections and extractions in contaminant transport, this paper explores the use of chaotic advection in two-phase flow systems. More specifically, we evaluate the effect of chaotic advection in the removal of NAPL using a five-spot injection-extraction well pattern in random heterogeneous porous media with different correlation structures and connectivities. To achieve this goal we have evaluated different synthetic cases where different scenarios of chaotic advection have been tested in two-phase flow systems. We have defined performance metrics to analyze the impact of chaotic flows on NAPL remediation, its effect on connectivity, and the role of heterogeneity and mobility ratio in chaotic flow configuration.

2 Methods

2.1 Chaotic Advection System

We evaluate an engineered chaotic advection system designed for extracting NAPL in a water-wet heterogeneous porous medium. Injection and extraction wells are organized to form a canonical five-spot pattern [*Satkin and Bedient*, 1988; *Juanes and Lie*, 2008]. This organization of wells is frequently used for extracting NAPL in contaminated sites [*Nicolaides et al.*, 2015], and oil in petroleum fields [*Craig*, 1971] as well as for carbon storage associated with CO_2 enhanced oil recovery (EOR) in residual oil zones [*Ren and Duncan*, 2019]. In the five-spot pattern, injection and extraction wells are uniformly distributed in such a way that each extraction well is surrounded by 4 injection wells, and an injection well is surrounded by 4 extraction wells (Figure 1). The wetting fluid is injected through the injection wells to displace the non-wetting fluid (NAPL) towards the central extraction well.

Let us denote the injection rate of the wetting fluid associated with the jth injection well of a given five-spot pattern as $Q^i_{w_j}(t)$, $j = \{1, 2, 3, 4\}$. Chaotic advection is generated by periodically fluctuating the injection rates $Q^i_{w_j}(t)$ in such a way that each injection well is out of phase with the others. In order to simplify the fluctuation system and reduce the number of parameters, we consider that injection rates follow a rectangular wave function with a time period T. This can be formulated by using the rectangular function f_j,

$$Q^i_{w_j}(t) = Q f_j(t, T), \qquad 0 \le t < T, \tag{1}$$

$$f_j(t, T) = H\left(t - (j-1)T/4\right) - H\left(t - jT/4\right), \tag{2}$$

together with the statement of periodicity,

$$Q^i_{w_j}(t) = Q^i_{w_j}(t - T), \qquad t \ge T, \tag{3}$$

where $H(\cdot)$ is the Heaviside function. Note that the rectangular function $f_j(t, T)$ is equal to 1 in the time interval $[jT/4 - T/4, jT/4]$ and zero otherwise. That is to say that the pulse duration τ is equal to $T/4$. Q is a constant value that specifies the injection rate of the wetting fluid when the well is active ($f_j = 1$). In short, the chaotic system set-up has two main features: (1) the injection rate is constant and equal to Q for a time interval $\tau = T/4$; and (2) each injection well is periodically activated with a period T. Thus, each injection period is divided into 4 equal subintervals of duration $T/4$. In each subinterval, only one injection well is active. That is, we first only activate the injection well 1 during the first time subinterval, while keeping the other injection wells deactivated. Then, we deactivate injection well 1 and only activate injection well 2 in the second time subinterval, and so on (see Figure 1).

2.2 Two-Phase Flow Model

We consider the movement of two immiscible liquids in a horizontal two-dimensional heterogeneous aquifer. Mass transfer (e.g., volatilization and dissolution) between the two liquid phases is assumed negligible. The governing equations used to simulate the two-phase flow system are determined by the mass conservation equation of the two liquids and the generalized Darcy's law. Assuming that the porous medium and the fluids are incompressible (constant porosity and fluid densities), we have the following coupled system of partial differential equations in two dimensions,

$$\phi b \frac{\partial S_w}{\partial t} = \nabla \cdot (\kappa \lambda_w b \nabla p_w) + \sum_{j=1}^{n_i} Q^i_{w_j}(t)\delta(\mathbf{x} - \mathbf{x}^i_j) - \sum_{j=1}^{n_e} Q^e_{w_j}(t)\delta(\mathbf{x} - \mathbf{x}^e_j), \tag{4}$$

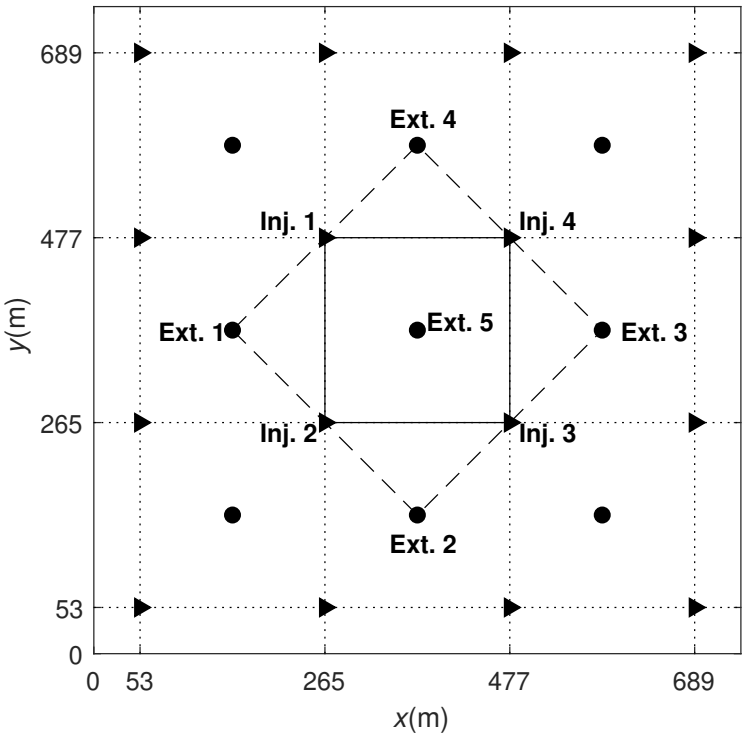

Figure 1: General five-spot arrangement of extraction and injection wells; the triangle symbols refer to the injection wells, whereas the circle symbols refer to the extraction wells; the region shown in solid lines is the domain of the synthetic test case TC1, and the region in dashed lines is the domain of the synthetic test case TC2.

$$\phi b \frac{\partial S_{nw}}{\partial t} = \nabla \cdot (\kappa \lambda_{nw} b \nabla p_{nw}) - \sum_{j=1}^{n_e} Q^e_{nw_j}(t)\delta(\mathbf{x} - \mathbf{x}^e_j), \tag{5}$$

where ϕ is the porosity, b is the aquifer thickness, $\mathbf{x} = (x, y)^t$, S_w and S_{nw} are the saturations of the wetting and the non-wetting fluids, $\delta(\cdot)$ is the Dirac delta function, n_i is the number of injection wells, n_e is the number of extraction wells, $\mathbf{x}^i_j$ is the position of the jth injection well, $\mathbf{x}^e_j$ is the position of the jth extraction well, κ is the intrinsic permeability, λ_w and λ_{nw} are the mobilities of the wetting and the non-wetting fluids, p_w and p_{nw} are the pressures of the wetting and the non-wetting fluids, $Q^i_{w_j}$ is the injection rate of the wetting fluid at the jth injection well, and $Q^e_{w_j}$ and $Q^e_{nw_j}$ are the extraction rates of the wetting and the non-wetting fluids at the jth extraction well. The total extraction rate associated with the jth extraction well is $Q^e_{t_j} = Q^e_{w_j} + Q^e_{nw_j}$. Fluid mobility is defined as the ratio of the relative permeability to the viscosity of the fluid,

$$\lambda_w = \frac{\kappa_{rw}}{\mu_w}, \qquad \lambda_{nw} = \frac{\kappa_{rnw}}{\mu_{nw}}, \tag{6}$$

where κ_{rw} and κ_{rnw} are the relative permeabilities of the wetting and the non-wetting fluids, and μ_w and μ_{nw} are the viscosities of the wetting and the non-wetting fluids. The relative permeabilities of the non-wetting κ_{rnw} and wetting κ_{rw} phases are only functions of water saturation and they are described by the Corey correlation model,

$$\kappa_{rnw} = \kappa_{rnwm}(1 - S_e)^{n_{nw}}, \tag{7}$$

$$\kappa_{rw} = \kappa_{rwm} {S_e}^{n_w}, \tag{8}$$

where κ_{rwm}, n_w, κ_{rnwm} and n_{nw} are the scaling parameters of the relative permeability curves, and S_e is the effective saturation of the wetting fluid defined as

$$S_e = \frac{S_w - S_{wr}}{1 - S_{wr} - S_{nwr}}, \tag{9}$$

where S_{wr} and S_{nwr} are the residual saturations of the wetting and the nonwetting phases, respectively. The extraction rate of the wetting and the non-wetting phase is determined by the fractional flow function $f_w(S_w)$ through

$$Q^e_{w_j} = Q^e_{t_j} f_w(S_w), \qquad Q^e_{nw_j} = Q^e_{t_j}\left(1 - f_w(S_w)\right), \tag{10}$$

where

$$f_w(S_w) = \frac{\lambda_w}{\lambda_w + \lambda_{nw}}. \tag{11}$$

The difference between the two fluid pressures defines the capillary pressure,

$$p_c = p_{nw} - p_w, \tag{12}$$

which is determined by the saturation-capillary pressure relationship or retention curve (see equation (16)). The system only considers the presence of two liquids and therefore the sum of saturations is equal to one, i.e., $S_w + S_{nw} = 1$.

2.3 Aquifer Heterogeneity

The intrinsic permeability and the retention curve are considered to vary in space. The natural log of the intrinsic permeability field, denoted as $Y(\mathbf{x}) = \ln \kappa(\mathbf{x})$, is considered to follow a stationary multi-Gaussian random distribution characterized by an exponential semi-variogram model of variance contribution σ_Y^2, defined as

$$\gamma(\mathbf{h}) = \sigma_Y^2 \left(1 - \exp\left(-3|\mathbf{h}'|\right)\right), \tag{13}$$

where $\mathbf{h}$ is the separation vector between two points of the aquifer, and $\mathbf{h}'$ is the separation vector obtained by orienting the correlation structure along the coordinates and scaling the ranges to unitary values according to

$$\begin{pmatrix} h'_x \\ h'_y \end{pmatrix} = \begin{pmatrix} \cos\theta & \sin\theta \\ -\sin\theta & \cos\theta \end{pmatrix} \begin{pmatrix} a_{\max}^{-1} & 0 \\ 0 & a_{\min}^{-1} \end{pmatrix} \begin{pmatrix} h_x \\ h_y \end{pmatrix}, \tag{14}$$

where $a_{\max}$ and $a_{\min}$ are the maximum and minimum ranges in the principal directions. The maximum correlation direction is oriented θ degrees counterclockwise from the positive x axis. The randomness of $Y(\mathbf{x})$ is transferred to the retention curve through the Leverett's function $J(S_e)$ [*Leverett*, 1939, 1941] that scales the capillary pressure via interfacial tension, porosity and intrinsic permeability [*Brown*, 1951; *Demond and Roberts*, 1991; *Lie*, 2014]. The Leverrett's function is an invariant property written as

$$J(S_e) = \frac{p_c}{\gamma \cos\alpha} \sqrt{\frac{\kappa}{\phi}}, \tag{15}$$

where γ is interfacial tension, and α is the contact angle. From this, assuming that the saturation-capillary pressure relation follows the *Brooks and Corey* [1966] model, the retention curve is assumed to vary as a function of the intrinsic permeability and the effective saturation by

$$p_c(S_e, \kappa) = p_L S_e^{-1/\lambda} \sqrt{\frac{\kappa_g}{\kappa}}, \qquad 0 < S_e \leq 1, \tag{16}$$

where p_L is the characteristic Leverett entry pressure, and κ_g is the geometric mean of permeability.

2.4 Fluid Mobility Ratio

The displacement of NAPL during injection not only depends on aquifer heterogeneity but also on the fluid properties [*Nicolaides et al.*, 2015]. The mobility ratio M is the mobility of the injection fluid divided by that of the non-wetting fluid it is displacing,

$$M = \frac{\kappa_{rw}^0 \mu_{nw}}{\mu_w \kappa_{rnw}^0}. \tag{17}$$

To estimate the mobility ratio, in accordance with *Craig* [1971], the relative permeability of the wetting fluid is defined with the average wetting fluid saturation $\overline{S}_{wBT}$ behind the displacing front at breakthrough (denoted as κ_{rw}^0), and the relative permeability of the non-wetting fluid is determined by the non-wetting fluid saturation ahead of the displacing front (denoted as κ_{rnw}^0), i.e., the initial saturation of NAPL. $\overline{S}_{wBT}$ is obtained by laying a tangent line to the fractional flow curve $f_w(S_w)$ from S_{wr} and extrapolating this tangent line to $f_w = 1.0$.

When $M < 1$ fluid displacement is said to have favorable mobility conditions. In this case, for a given pressure gradient, the wetting fluid can travel at a lower velocity than the non-wetting fluid, effectively pushing the NAPL towards extraction wells. On the contrary, when $M > 1$ the wetting fluid can travel faster than the non-wetting fluid and there is a tendency for the NAPL to be bypassed. During the in situ remediation of a contaminated aquifer, liquid solutions with chemicals (e.g., surfactants, alkalis, or polymers) are sometimes injected into the aquifer to improve field conditions by decreasing the mobility ratio M [*Huling and Weaver*, 1991]. Similar strategies are often used in petroleum engineering to enhanced oil recovery [*Abidin et al.*, 2012; *Raffa et al.*, 2016]. Here, we analyze the effect of the mobility ratio on the performance of chaotic advection by changing the viscosity of the wetting fluid so as to represent favorable and unfavorable mobility conditions. Thus, we consider three different mobility ratios, i.e., M = 0.5, 1.4, and 2.2. Considering that NAPL viscosity (e.g., Chlorohydrocarbons and oil products) typically ranges from 0.35 to 28 [mPa·s] [*Schwille*, 1981; *Huling and Weaver*, 1991; *Reid et al.*, 1997; *Boulding*, 1996], approximately equivalent to a mobility ratio ranging between 0.1 and 1.8, these values cover a wide range of applications.

2.5 Synthetic Test Cases

The objective of the synthetic test cases is to compare chaotic advection NAPL removal with a constant injection scheme in complex geological formations. The effect of chaotic advection is studied in a wide variety of permeability fields. For this, we consider two synthetic test cases, denoted as TC1 and TC2, that respectively represent two heterogeneous aquifers with different correlation structure of the permeability field and hydraulic connectivity between injection and extraction wells. Let us consider the general arrangement of injection and extraction wells shown in Figure 1. The distance between two adjacent injection or extraction wells is 212 m and the aquifer thickness is 20 m. The aquifer system is assumed to be initially filled with residual water $S_{wr} = 0.2$ and a large amount of NAPL. The injection-extraction system operates over 20 years. The model domain of TC1, denoted as V_1, is delimited by the inner square region shown in Figure 1. This test case involves 4 injectors and 1 central extraction well. TC1 represents a generic five-spot injection-extraction system embedded in an isotropic two dimensional heterogeneous $Y(\mathbf{x})$ field with $a_{\max} = a_{\min} = 51$ m. The model domain of TC2 is defined by the dashed lines shown in Figure 1. The domain contains 5 extraction wells and 4 injectors. TC2 represents the same five-spot pattern but in this case the injection-extraction system is embedded in an anisotropic heterogeneous $Y(\mathbf{x})$ field with $a_{\max} = 225$ m, $a_{\min} = 22.5$ m, and $\theta = 45°$. The maximum correlation direction is oriented along the line connecting injection and extraction wells to enhance hydraulic connectivity. The maximum range is smaller than the field scale to assure the effect of permeability heterogeneity is activated; otherwise, the field is relatively homogeneous. The two heterogeneous systems share the same geometric mean of the intrinsic permeability, $\kappa_g = 10^{-14}$ m^2, and we explore three different degrees of heterogeneity, σ_y^2 = 0.1, 2, and 6, which represent a mild, moderate, and highly heterogeneous aquifer. We chose to work with a low κ_g value to test chaotic advection under adverse conditions with permeability values that fluctuate between 10^{-18} and 10^{-10} m^2. NAPL is typically difficult to recover in low permeability formations [*Mackay and Cherry*, 1989]. We note though that the analysis is presented using dimensionless variables to make the results more general. The geostatistical parameters of the $Y(\mathbf{x})$ random fields are summarized in Table 1.

All domain boundaries are set to no-flow conditions. The extents of V_1 and V_2 are 212×212 m^2 and 300×300 m^2, respectively. V_2 is larger than V_1 to allow aligning the domain boundaries with the stratification in the TC2 case. Note that, otherwise, the injected fluid would be forced to move through the stratification. Of course, some boundary effects are expected but the intend here is not to exactly reproduce a large field system but to compare chaotic advection removal with a conventional scheme. The total extraction rate assigned to the central well is always constant and fixed to $Q^e_{t_5} = Q$ in all cases. Chaotic advection follows always a rectangular wave function with amplitude Q and period T. The constant injec-

tion scheme considers that $Q^i_{w_j} = Q/4$ in TC1 and $Q^i_{w_j} = Q/2$ in TC2 for $j = \{1, 2, 3, 4\}$. In TC2, the total extraction rate of corner wells are fixed to $Q^e_{t_j} = Q/4$ for $j = \{1, 2, 3, 4\}$. Parameters adopted during the simulations are listed in Table 1. The domains of TC1 and TC2 are respectively discretized into 101 and 201 squared cells to represent the variability of the random fields. The resolution of the random fields vary between 15 and 150 cells per range, which is considered sufficient to represent the inherent spatial variability of permeability. Figure 2 shows illustrative test fields and corresponding well arrangements. To improve visualization, TC2 is rotated 45° clockwise from the x positive axis.

The simulation approach is as follows. For each test case, we first consider a stochastic description of $Y(\mathbf{x})$ with 100 equally likely realizations characterized by $\sigma^2_Y = 2$ and $M = 2.2$ to explore the range of uncertainty. Within each realization, two-phase flow simulations with constant-injection and chaotic advection removal are conducted with different periods T, which vary from 0.5 to 20 years. Performance metrics are then characterized by their statistical moments (mean behavior and uncertainty) and sample probability density functions (PDFs). Finally, we investigate the effect of the degree of heterogeneity σ^2_Y and mobility ratio M in individual realizations. The effect of σ^2_Y is analyzed by re-scaling the variance of the $Y(\mathbf{x})$ values adopted in a given realization so as to always replicate the same specific heterogeneous patterns. The viscosity of the non-wetting fluid is kept constant to 13 mPa·s, while the viscosity of the wetting fluid is changed from 1.0 to either 0.2 or 5.0 mPa·s (see Table 1), which can represent, for instance, chemical flooding with polymers during NAPL remediation or enhanced oil recovery with CO_2 sequestration, respectively.

Random fields are generated with the Sequential Gaussian Simulation method implemented in the SGSIM code [*Journel and Huijbregts*, 1976]. We use the open-source Matlab Reservoir Simulation Toolbox (MRST)[*Krogstad et al.*, 2015] to simulate two-phase flow using the IMplicit Pressure Explicit Saturation (IMPES) algorithm [*Lie*, 2014; *Chen et al.*, 2006; *Yanosik and McCracken*, 1979]. The numerical discretization of the flow solution and the $Y(\mathbf{x})$ field is the same. The maximum time step for updating saturation is constraint by the Courant-Friedrichs-Lewy (CFL) condition to assure that the time step for updating saturation is smaller than that for updating pressure [*Courant et al.*, 1928; *Coats*, 2003]. The two-point flux approximation (TPFA) is employed to solve the pressure equation. The one-point upstream weighting scheme is used to avoid artificial dispersion [*Forsyth and Sammon*, 1986; *Sammon*, 1988; *Allen*, 1985]. This upstream weighting scheme has first-order spatial accuracy [*Sleep and Sykes*, 1993a,b].

2.6 Performance Metrics

We define two different performance metrics to evaluate the relative efficiency of the proposed chaotic advection system involved in a five-spot pattern: the removal efficiency and the saturation distribution index. The removal efficiency $RE(t)$ measures the volume of NAPL recovered at time t relative to the initial volume of NAPL in the aquifer, and the distribution index $DI(t)$ quantifies the degree of uniformity of the wetting fluid saturation distribution at time t [*Le Borgne et al.*, 2010; *Nicolaides et al.*, 2015]. The formal definition of these metrics can be written as,

$$RE(t) = \frac{1}{V_{nwi}} \int_0^t Q_{nw_5}(t) dt, \tag{18}$$

$$DI(t) = 1 - \frac{\sigma^2(t)}{\sigma^2_{\max}(t)}, \tag{19}$$

where Q_{nw_5} is the NAPL extraction rate obtained at the central well of the five-spot pattern (see Figure 1), V_{nwi} is the initial volume of NAPL in the V_1-domain,

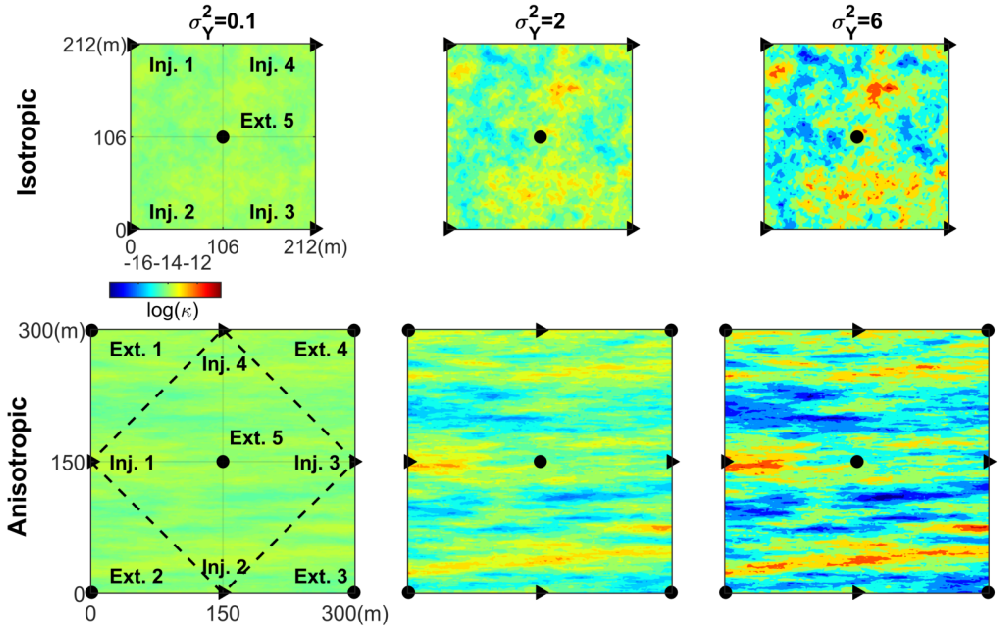

Figure 2: Test fields and corresponding well arrangements; the first panel of the figure shows one realization of the isotropic random field used in the synthetic test case TC1, and the second panel shows one realization of the anisotropic random field used in the synthetic test case TC2 (the domain has been rotated 45° clockwise from the x positive axis to improve visualization).

Table 1: Summary of the parameters adopted during the simulations for the two synthetic test cases.

Parameters	**TC1**	**TC2**	References
(n_e, n_i) [-]	(1, 4)	(5, 4)	*Craig* [1971]
V [m^3]	$212 \times 212 \times 20$	$300 \times 300 \times 20$	-
$n_x \times n_y \times n_z$[-]	101×101	201×201	-
κ_g [m^2]	10^{-14}	10^{-14}	*Mackay and Cherry* [1989]; *Wu et al.* [1994]
σ_Y^2 [-]	0.1 / 2.0 / 6.0	0.1 / 2.0 / 6.0	*Craig* [1971]; *Dillard et al.* [1997]
$(a_{\max}, a_{\min})$ [m]	(51, 51)	(225, 22.5)	*Kitanidis* [1997]
θ [degrees]	0°	45°	-
ϕ [-]	0.2	0.2	*Wu et al.* [1994]
Q [10^{-3}m^3/s]	0.228	0.228	-
(ρ_{nw}, ρ_w) [kg/m^3]	(898, 981)	(898, 981)	*Schwille* [1981]
μ_{nw} [mPa· s]	13.0	13.0	*Schwille* [1981]
μ_w [mPa· s]	0.2 / 1.0 / 5.0	0.2 / 1.0 / 5.0	*Schwille* [1981]
M [-]	2.2 / 1.4 / 0.5	2.2 / 1.4 / 0.5	*Schwille* [1981]
(S_{wr}, S_{nwr}) [-]	(0.2, 0.2)	(0.2, 0.2)	*Wu et al.* [1994]; *Lie* [2014]
$(\kappa_{rwm}, \kappa_{rnwm})$ [-]	(0.2, 0.8)	(0.2, 0.8)	*Craig* [1971]; *Lie* [2014]
(n_w, n_{nw}) [-]	(2, 2)	(2, 2)	*Sleep and Sykes* [1993a]
p_L [Pa]	8^a	8	*Zhong et al.* [2001]; *Wipfler et al.* [2004]
λ [-]	0.5	0.5	*Sleep and Sykes* [1993a]

[a] Low entry pressure is used considering the imbibition process.

$$V_{nwi} = \int_{V_1} \phi S_{nw}(t=0) dV, \tag{20}$$

σ^2 is the variance of the S_w-distribution in the V_1-domain, and $\sigma^2_{\max}$ is the maximum variance of S_w in the V_1-domain. The variance of saturation associated with the wetting fluid is defined as

$$\sigma^2(t) = \frac{1}{V_1}\int_{V_1} S_w^2(t) dV - \left(\frac{1}{V_1}\int_{V_1} S_w(t) dV\right)^2. \tag{21}$$

Note that the performance metrics only consider the simulated values obtained in the V_1 region. This intends to minimize boundary effects in TC2. The maximum variance $\sigma^2_{\max}$ is obtained when the distribution of saturation (wetting fluid) exhibits a bimodal distribution with two segregated modes. In a multiphase injection-extraction removal system, this happens at early stages after injection, when the displacement is piston-like and the saturation of the injected fluid behind the displacement front is significantly different from the saturation ahead, which is close to the initial saturation. With time, driven by capillary dispersion and heterogeneity (and in our case chaotic advection), these two distinct saturations will mix. In an ideal case, when the saturation distribution is perfectly mixed, the saturation distribution approaches a unimodal distribution with $\sigma^2 = 0$ and $DI = 1$. Similar metrics of mixing (substituting S_w by solute concentrations) can be found in the literature of solute transport in porous media [*Jha et al.*, 2011]. Here, knowing that S_w ranges between 0 and 1, we estimated $\sigma^2_{\max}$ by the following upper bound of variance [*Bhatia and Davis*, 2000],

$$\sigma^2_{\max}(t) = \frac{1}{V_1}\int_{V_1} S_w(t)dV - \left(\frac{1}{V_1}\int_{V_1} S_w(t)dV\right)^2. \tag{22}$$

The chaotic advection system results are compared with a standard injection-extraction removal system characterized by constant injection rates. Whenever necessary for a better interpretation of the results, performance metrics are presented as fractional increase with respect to the constant-injection solution. For any given performance metric χ, the fractional increase of χ is determined as

$$\Delta\chi = \frac{\chi_c - \chi_r}{\chi_r}, \tag{23}$$

where the subscripts c and r denote the chaotic advection and the reference constant injection rate simulation results, respectively.

2.7 Dimensionless Variables

To facilitate the interpretation, we present the results in terms of dimensionless variables. In statistical physics, the Kubo number Ku is a dimensionless measure of the correlation time of the fluctuations typically used for analyzing the behavior of moving particles in turbulent, random or chaotic velocity fields [*Kubo*, 1963; *Mazzino*, 1997; *Castiglione*, 2000; *Vlad et al.*, 2001]. The Kubo number has been also used to study solute transport in temporally fluctuating flow through randomly heterogeneous porous media [*Dentz and Carrera*, 2005; *De Dreuzy et al.*, 2012]. In solute transport, the Kubo number compares the average travel distance of a particle with the integral scale of $Y(\mathbf{x})$. Here, based on this, we define the following Kubo number in two-phase flow systems subject to periodic injection pulses,

$$\mathrm{Ku} = \frac{v_f \tau}{\ell}, \tag{24}$$

where τ is the pulse duration, v_f is the mean velocity of the saturation front, and ℓ is a measure of the correlation scale of $Y(\mathbf{x})$. The mean velocity of the saturation front is estimated by the breakthrough time of the saturation of the wetting fluid at the central extraction well of the five-spot pattern under constant injection conditions, denoted as t_{BT},

$$v_f \approx \frac{L}{\langle t_{BT}\rangle}, \tag{25}$$

where L is the separation distance between injection and extraction wells, and $\langle\cdot\rangle$ denotes the ensemble average of the Monte Carlo simulations. Note that this way the Kubo number directly includes the breakthrough time, which is known to control the efficiency of NAPL removal in real applications. Here, we choose to use the range of the $Y(\mathbf{x})$ field as a measure of correlation because it provides an indication of the average extent of low/high permeability zones. Since in our chaotic removal setup the injected fluid moves half of the time along and transverse to the direction of stratification in an average sense, we have used $\ell = (a_{\max} + a_{\min})/2$ to estimate the Kubo number. We have also normalized the time by

$$t^* = \frac{v_f t}{\ell}. \tag{26}$$

The number of cycles completed after a time t during chaotic advection removal is defined as $N = t/T$. Dividing (26) by (24) and knowing that $T = 4\tau$, we have

$$N = \frac{t^*}{4\mathrm{Ku}}. \tag{27}$$

In the appendix we show that the governing equations of the two-phase flow system considered can be written in a dimensionless form that directly depends on the Kubo number and these dimensionless variables.

In a given realization of the random field, we expect the hydraulic connectivity between injection and extraction wells to control the efficiency of the injection-extraction system; high connectivity can generate fast flow pathways between injection and extraction wells leading to early breakthrough times [*Silliman and Wright*, 1988; *Labolle and Fogg*, 2001; *Bianchi et al.*, 2011b; *Renard and Allard*, 2013b; *Edery et al.*, 2014]. Several indicators of connectivity have been proposed in subsurface hydrology for flow and contaminant transport in aqueous phase systems [*Sánchez-Vila et al.*, 1999; *Fernàndez-Garcia et al.*, 2002; *Knudby and Carrera*, 2005; *Trinchero et al.*, 2008]. Here, following *Fernàndez-Garcia et al.* [2010], we define an indicator of point-to-point connectivity for multiphase flow systems as,

$$CS = \frac{t_0}{t_{BT}}, \tag{28}$$

where t_0 is an expected or reference value of the saturation breakthrough time. Injection and extraction wells are well connected in terms of saturation displacement when $CS > 1$, since the observed breakthrough time is more rapid than that its expected reference value. The larger the CS value, the better connection exists between injection and extraction wells, and one should expect geological bodies of high permeability connecting injection and extraction wells. We chose to measure t_0 by the expected value of the breakthrough time of saturation $\langle t_{BT} \rangle$ obtained in isotropic random fields under constant injection conditions.

3 Results and Discussions

3.1 Mean Behavior: The Role of the Fluctuation Period

The ensemble averages of the fractional increase of the removal efficiency $\langle \Delta RE \rangle$ and distribution index $\langle \Delta DI \rangle$ are shown in Figure 3 as a function of the Kubo number for different removal times. Here, we only employ chaotic periods smaller than the total recovery time to assure that chaotic advection is active, otherwise the flow is effectively steady. Results show that $\langle \Delta RE \rangle$ increases to a maximum value when a specific pulse duration τ of a periodically applied rotating injection pulse yields a Kubo number close to one, i.e., Ku $\approx$ 1. This result is somehow analogous to the effect of temporal flow fluctuations on solute transport (single phase). *Dentz and Carrera* [2005] and *De Dreuzy et al.* [2012] found that the effective transverse dispersion coefficient of a solute plume is maximized when Ku = 1. This suggests that in a two-phase flow system, when Ku = 1, advective transport and temporal fluctuations are synchronized to improve NAPL displacement towards the extraction well, most likely due to an enhancement of transverse dispersion of the displacing fluid saturation. In practice, this means that the saturation front should travel one range of the $Y(\mathbf{x})$ field (an average extent of low/high permeability zones) in an injection pulse to maximize NAPL removal. When Ku$\ll$1, the frequency of temporal fluctuations is too high to properly sample the permeability field. When Ku$\gg$1, chaotic advection generates a highly nonuniform partial sweep of the porous medium.

Remarkably, a more pronounced peak is observed in the anisotropic case, which suggests that chaotic removal works best under unfavorable field conditions, i.e., when some of the injectors are potentially correlated with the central well. In the anisotropic case we obtain a maximum fractional increase close to 12%, which is six times larger than that of the isotropic case. In particular, the pulse duration for maximizing removal efficiency in TC1 and TC2 are $\tau \approx \langle t_{BT} \rangle/5$ and $\tau \approx \langle t_{BT} \rangle/2$, respectively. It is logical to think that the pulse duration should be smaller than the breakthrough time, otherwise the wetting fluid can gain access to the extraction well in the first injection of the fluctuation cycle. Following this line

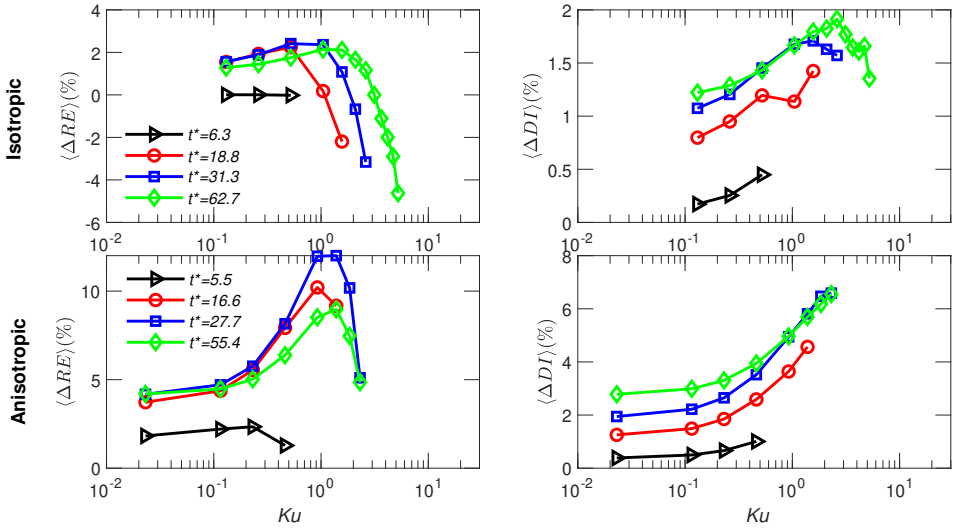

Figure 3: Ensemble average of the fractional increase of the removal efficiency and distribution index as a function of the Kubo number for different removal times in isotropic (first panel) and anisotropic (second panel) random permeability fields with $\sigma_Y^2 = 2$ and $M = 2.2$.

of thought, it is not surprising that $\langle \Delta RE \rangle$ rapidly declines after passing through a maximum when the pulse duration, and therefore the Kubo number, becomes too large ($\langle \Delta RE \rangle$ can reach negative values in the isotropic case).

The ensemble average of the fractional increase of the distribution index $\langle \Delta DI \rangle$ is also shown in Figure 3. Chaotic advection is also demonstrated to enhance mixing. However, a clear peak is only observed in the isotropic case after a long time (when $t^* > 15$) and at Kubo numbers slightly larger than 1 (between 1.5 and 3). Probably, the peak cannot be seen in the other cases because the maximum Kubo number available is relatively small. These results highlights that maximum mixing does not necessarily imply maximum removal, most likely because the wetting fluid can only effectively displace the non-wetting fluid when $S_w \gg S_{wr}$ due to the non-linear nature of the relative permeability.

Figure 4 depicts the temporal evolution of $\langle \Delta RE \rangle$ and $\langle \Delta DI \rangle$ for different Kubo numbers. Chaotic effects on $\langle \Delta RE \rangle$ require a certain time to develop during which sometimes it exhibits a valley, then reaches a maximum, and after this it slowly declines with time. These features are more intense for anisotropic fields. The valley displays negative values decreasing with the Kubo number. In general, the time needed to reach the valley and the peak is relatively smaller in anisotropic fields, meaning that chaotic advection effects develop faster in well-connected permeability fields. From (27), we have that $N = t^*/4$, which means that the number of cycles require to reach maximum removal is only about 2 and 3 cycles in the anisotropic and isotropic case, respectively. The valley seems to take place in the first cycle. From a practical point of view, it is important to recognize that these results suggest that in order to maximize removal in the long term one should undergo first an early stage with detrimental effects in removal efficiency. The temporal evolution of $\langle \Delta DI \rangle$ is similar to $\langle \Delta RE \rangle$, but in this case the valley and the peak take place at different times and with less intensity. In fact, the valley becomes only apparent when Ku > 1.

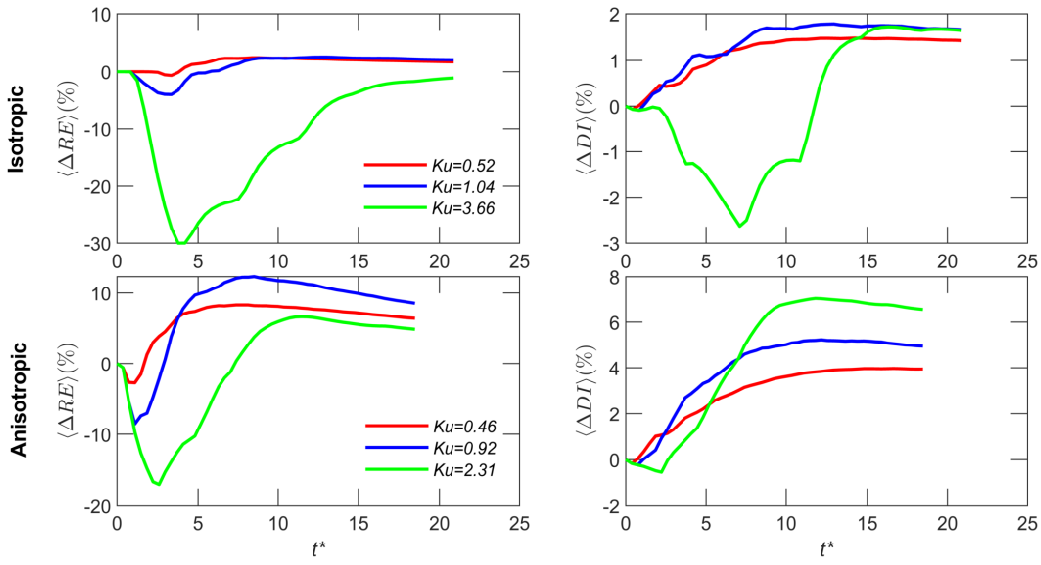

Figure 4: Temporal evolution of the ensemble average of the fractional increase of removal efficiency and distribution index for different Kubo numbers in isotropic (first panel) and anisotropic (second panel) random permeability fields with $\sigma_Y^2 = 2$ and $M = 2.2$.

3.2 Uncertainty in Chaotic Advection NAPL Removal

The inherent complexity of a heterogeneous geological system typically produces large uncertainties in the efficiency of NAPL removal in field applications. For instance, it is well known that DNAPL removal efficiencies of current remediation techniques are limited and highly variable when moving from laboratory to field scale [*Soga et al.*, 2004]. In this section, we demonstrate that chaotic advection removal not only improves performance metrics, but also reduces uncertainty, making the application of in situ removal techniques more reliable and less sensitive to the underlying heterogeneity of the permeability field. To show this, Figure 5 presents the coefficients of variation of the removal efficiency CV_{RE} and distribution index CV_{DI} as a function of the Kubo number for different removal times. For comparison purposes, the horizontal dashed lines shown in the figures indicate the corresponding coefficient of variation obtained with a constant injection scheme. In general, the coefficient of variation of RE is one order of magnitude larger than that of DI. Results demonstrate that chaotic removal can significantly reduce the uncertainty of removal efficiency and distribution index relative to a constant injection scheme. This effect is more pronounced in the anisotropic case with unfavorable conditions. In this case, the coefficients of variation of RE and DI are respectively reduced from 0.15 to 0.12 and from 0.023 to 0.008. The uncertainty in removal efficiency exhibits its minimum value when $\langle \Delta RE \rangle$ is maximum (Ku $\approx$ 1). This suggests that the increase in removal efficiency and distribution index due to chaotic advection always goes along with a reduction of their uncertainty.

The temporal evolution of the coefficient of variation of performance metrics is depicted in Figure 6 for different Kubo numbers. For comparison, the dashed lines correspond to the constant injection scheme. In general, the uncertainty of RE and DI exhibits large fluctuations at early times, which ultimately vanish to approach a well-defined asymptotic value at large times. The effects of chaotic advection are more pronounced in the anisotropic case with similar overall behavior. The time needed to reach an asymptotic value in removal

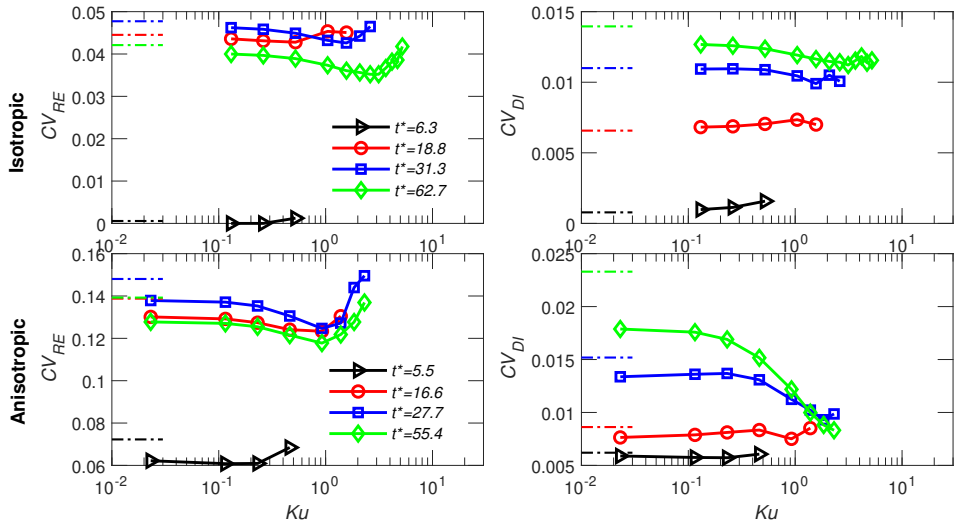

Figure 5: Coefficient of variation of the removal efficiency and distribution index as a function of the Kubo number for different removal times in isotropic (first panel) and anisotropic (second panel) random permeability fields with $\sigma_Y^2 = 2$ and $M = 2.2$.

efficiency strongly depends on the Kubo number. When Ku $\approx$ 1, CV_{RE} approaches the asymptotic value more rapidly than in other cases, i.e., in less than one range of the $Y(\mathbf{x})$ field. The coefficient of variation of the distribution index, at late times, decreases with the Kubo number. This illustrates that low-frequency fluctuations can further reduce the uncertainty of mixing but at the expenses of removal efficiency and its uncertainty.

The probability density function (PDF) of RE and DI provides a broader description of the ensemble of realizations. This is shown in Figure 7 for a removal time of 10 years. We compare the results obtained by using a constant injection with those obtained by using chaotic advection with optimal Kubo number. The PDFs were estimated through an iterative optimal kernel density estimator [*Engel et al.*, 1994] to minimize spurious statistical fluctuations. As expected from our previous results, the central tendency of the PDFs is shifted towards larger removal efficiencies and distribution indexes due to chaotic advection. In a constant injection scheme, removal efficiency exhibits a wide distribution with a long tail associated with relatively large removal efficiencies. In contrast, NAPL removal with chaotic advection yields a more symmetric and narrower distribution of the removal efficiency with high probabilities centered at relatively large quantities.

3.3 Impact of Chaotic Advection on Connectivity

The hydraulic connection between injection and extraction wells depends on the specific spatial patterns that the permeability field displays in a given realization. Within each realization, the measure of connectivity CS presented in section 2.7 quantifies the presence of preferential channels or high permeability regions between injection wells and the central extraction well [*Trinchero et al.*, 2008; *Fernàndez-Garcia et al.*, 2010]. Within this context, in this section we analyze the dependence between chaotic removal and connectivity. For this, we present in Figure 8 the conditional expectation of the removal efficiency and distribution index (and corresponding fractional increase) relative to the connectivity indicator,

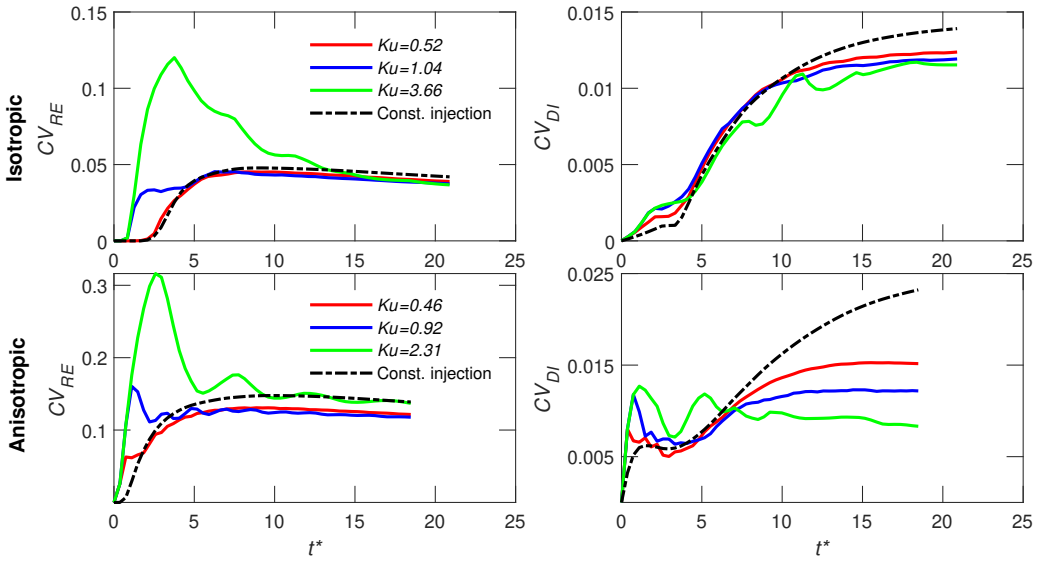

Figure 6: Temporal evolution of the coefficient of variation of the removal efficiency and distribution index as a function of the Kubo number for different removal times in isotropic (first panel) and anisotropic (second panel) random permeability fields with $\sigma_Y^2 = 2$ and $M = 2.2$.

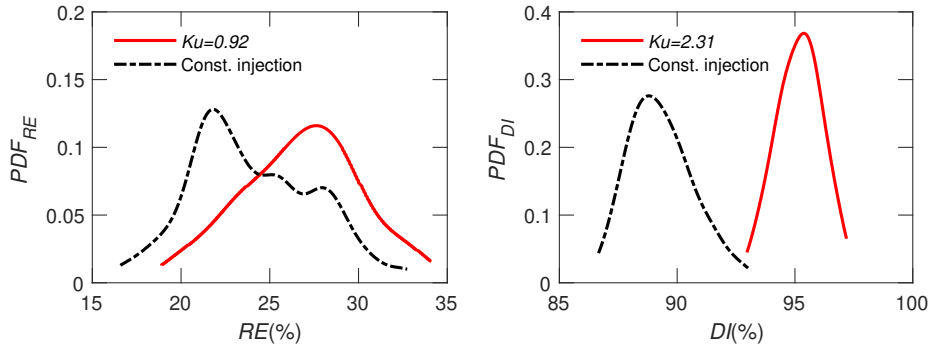

Figure 7: Comparison of the estimated probability density functions of the removal efficiency and distribution index obtained with chaotic advection (Kubo numbers associated with maximum performance) and constant injection removal for anisotropic fields with σ_Y^2=2 and M=2.2 after 10 years of operation.

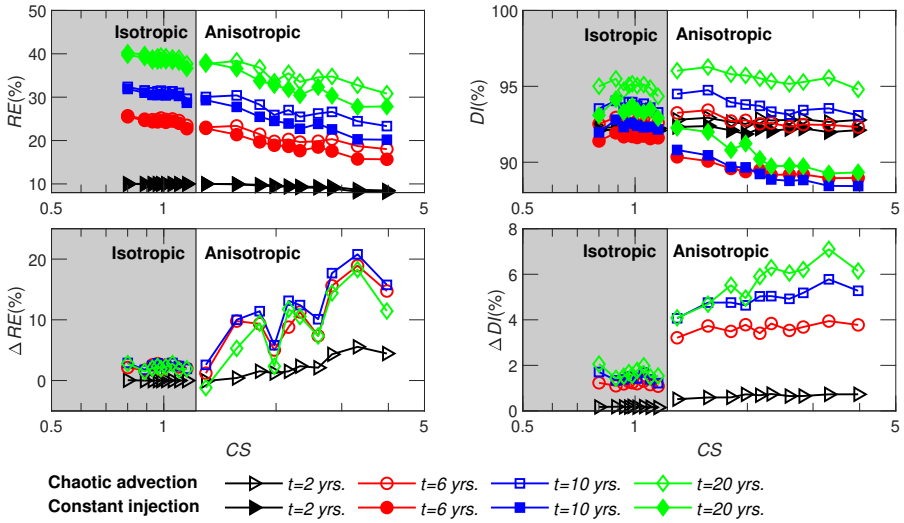

Figure 8: Removal efficiency and distribution index (and their corresponding fractional increase) as a function of point-to-point connectivity in two-phase flow systems for different removal times and injection-extraction method in isotropic and anisotropic random fields with $\sigma_Y^2 = 2$ and $M = 2.2$.

i.e., $\langle RE|CS\rangle$ and $\langle DI|CS\rangle$, for different removal times. Here, the pulse duration is chosen to satisfy maximum performance.

Results agree with field observations in that removal efficiency decreases with connectivity. The inefficiency of NAPL removal is mainly attributed to the inability of the displacing fluid to sweep the NAPL trapped in low permeability regions, which is bypassed when the injection and extraction wells are well connected [*De Dreuzy et al.*, 2012; *De Barros et al.*, 2013; *Edery et al.*, 2014]. As expected, the anisotropic random fields reflect large CS values (Figure 2). TC2 exhibits elongated lenses of high/low permeabilities between the injectors and the central extraction well. Looking at both the removal efficiency and its fractional increase we see that even though the removal efficiency decreases with connectivity, the fractional increase due to chaotic advection becomes important with increasing CS. That is, the fractional increase of the removal efficiency increases with unfavorable connectivity conditions, meaning that chaotic removal works best in the worst case scenario. Hence, to some extent, results suggest that chaotic advection can partially overcome channeling effects during NAPL removal.

Connectivity affects the distribution index (mixing of saturations) in a similar way. Recalling that the distribution index is a measure of mixing, results indicate that strong connectivity patterns in a heterogeneous aquifer tend to preclude the occurrence of mixing. It is logical to think that well-connected fields will concentrate the wetting fluid in small regions, making it difficult for mixing to occur [*De Barros et al.*, 2013]. This is equally true for both injection modes, but one can easily appreciate that chaotic removal renders the system less dependent on connectivity, because the chaotic advection can partially break fast flow paths. Similar effects have been reported in solute transport [*De Dreuzy et al.*, 2012]. DI decreases with CS but at a smaller rate during chaotic advection removal.

3.4 The roles of the Degree of Heterogeneity and Mobility Ratio

In this section we evaluate the roles that heterogeneity and mobility ratio have on removal efficiency and mixing. The effect of σ_Y^2 is analyzed by re-scaling the variance of the $Y(\mathbf{x})$ values adopted in a given realization. A similar approach was used by [*Neupauer et al.*, 2014]. This way we make sure that we always deal with the same heterogeneous pattern, i.e., the same organization of permeability values. The $Y(\mathbf{x})$ fields used are shown in Figure 2. We also changed the viscosity of the wetting fluid to analyze the effect of the mobility ratio on chaotic removal. The mobility ratio is changed from $M = 2.2$ to $M = 1.4$ and $M = 0.5$. Figure 9 shows the fractional increase of removal efficiency obtained in the isotropic and anisotropic case after 20 years as a function of the Kubo number for different σ_Y^2 and M values. The general behavior follows our previous results; maximum removal close or slightly larger than Ku $\approx$ 1 followed by a rapid decline. The location of the peak slightly depends on the mobility ratio, indicating that unfavorable displacement ($M > 1$) may require slightly smaller frequencies of chaotic fluctuations. However, the important point here is to realize that chaotic removal in two-phase flow systems is significantly affected by two competing factors: mobility ratio and heterogeneity. When the degree of heterogeneity is not significant ($\sigma_Y^2 < 2$), the unfavorable displacement caused by high mobility ratios controls removal efficiency, i.e., ΔRE increases with the mobility ratio. When heterogeneity is important ($\sigma_Y^2 > 2$), channeling controls the displacing process regardless of the mobility ratio. We note also that chaotic advection is more effective under unfavorable conditions of heterogeneity, i.e., high σ_Y^2 in well-connected anisotropic fields. This is because removal efficiency is typically small in highly heterogeneous systems due to channeling, thus leaving a large opportunity for improvement. In this case, for this realization of the random field, we obtain a fractional increase larger than 20% at peak values. In this context, we note that *Neupauer et al.* [2014] also found that chaotic advection in solute transport (single phase) is most advantageous in highly heterogeneous fields with large σ_Y^2.

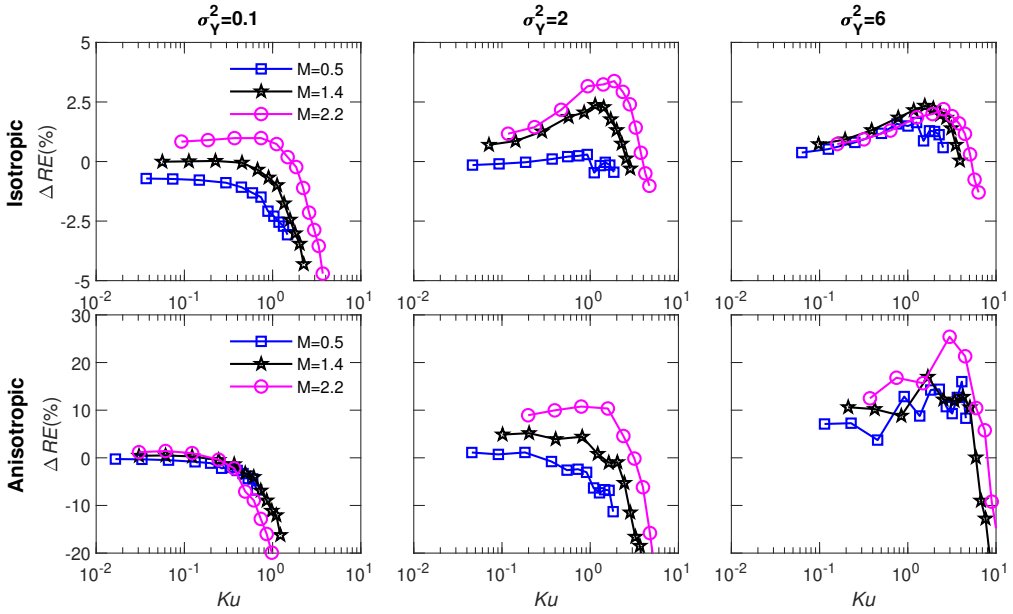

Figure 9: Fractional increase of the removal efficiency as a function of the Kubo number for different degrees of heterogeneity and mobility ratios in one realization of the isotropic (first panel) and anisotropic (second panel) random field.

To visually illustrate the benefits of chaotic advection removal, Figures 10 and 11 offer the map of the wetting fluid saturation after 20 years of operation in the isotropic and anisotropic permeability fields shown in Figure 2 for $M = 2.2$ and $\sigma_Y^2 = 0.1$, 2, and 6. Constant injection results are compared with those corresponding to the chaotic sequences that yielded maximum removal (RE) and maximum mixing (DI). We can easily see that chaotic removal with optimal fluctuations can significantly outperform the constant injection scheme. This is particularly notable when field conditions are unfavorable, i.e., large σ_Y^2 and injection-extraction wells oriented along the principal correlation direction. Note for instance that even though severe stratification (anisotropic case with σ_Y^2=6) controls the distribution of saturation in a constant injection scheme, the application of chaotic advection can largely palliate this shortcoming. This figure also illustrates the dichotomy between maximizing removal efficiency or mixing. Results have shown that these two conditions occur at different chaotic periods and removal times. In practice, the use of one or another will depend on the project objectives. For instance, at early stages of remediation one may favor removal efficiency, but at late times, when liquid solutions with cosolvents, surfactants or polymers are meant to be used to alter fluid properties and improve performance, one may wish to promote mixing [*Huling and Weaver*, 1991; *Rao et al.*, 1997; *Neupauer et al.*, 2014].

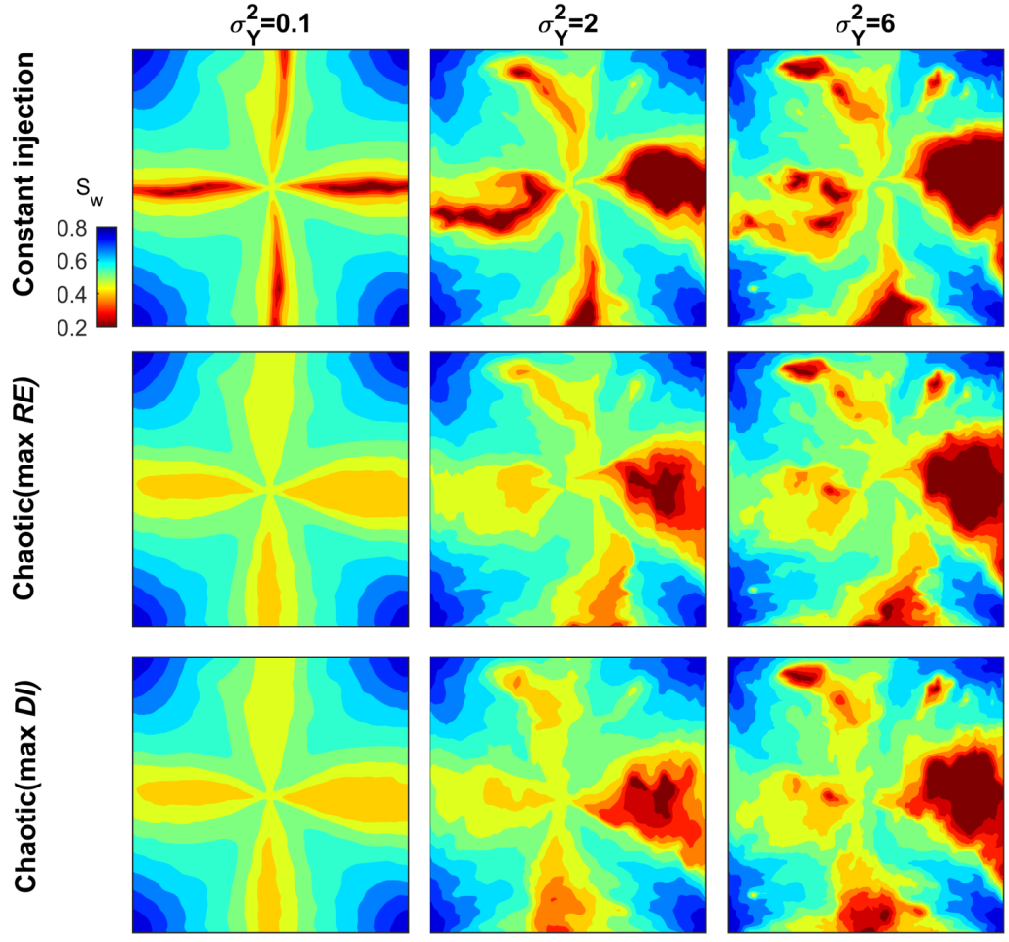

Figure 10: Spatial distribution of the wetting fluid saturation after 20 years of operation in one realization of the isotropic random field for different degrees of heterogeneity and injection-extraction method with M=2.2.

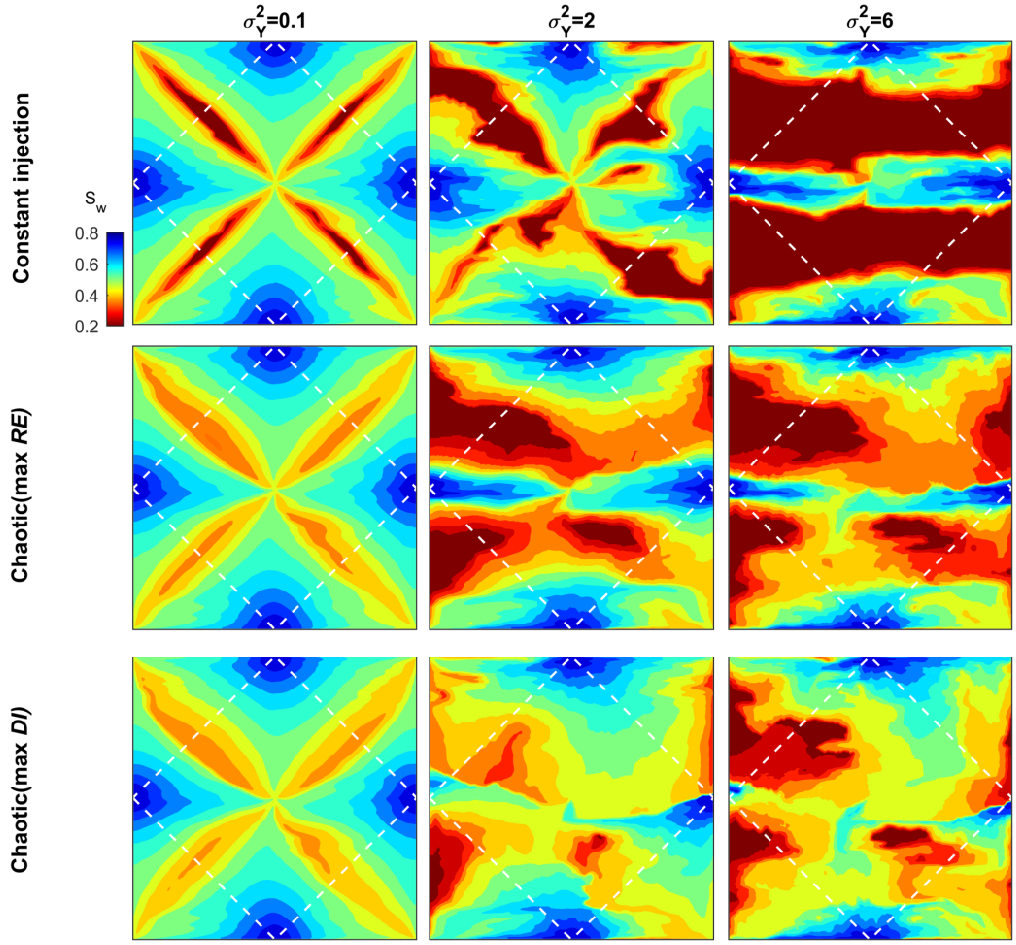

Figure 11: Spatial distribution of the wetting fluid saturation after 20 years of operation in one realization of the anisotropic random field for different degrees of heterogeneity and injection-extraction method with M=2.2.

As an illustrative example of the method, we finally compare in Figure 12 the temporal evolution of the NAPL flow rate recovered at the central well of the five-spot pattern produced by chaotic advection with that of the constant injection scheme obtained in a given realization of the anisotropic permeability field for σ_Y^2=6 and $M = 2.2$ (worst case scenario). Once the non-wetting fluid breaks through the extraction well, the fractional flow rate of NAPL rapidly declines, generating a long tail of poor removal efficiencies with time. Instead, enhanced NAPL removal with chaotic advection produces a more persistent NAPL extraction rate sequence characterized by important NAPL removal spikes. The net result in this case is a relative increase in removal efficiency of 22%.

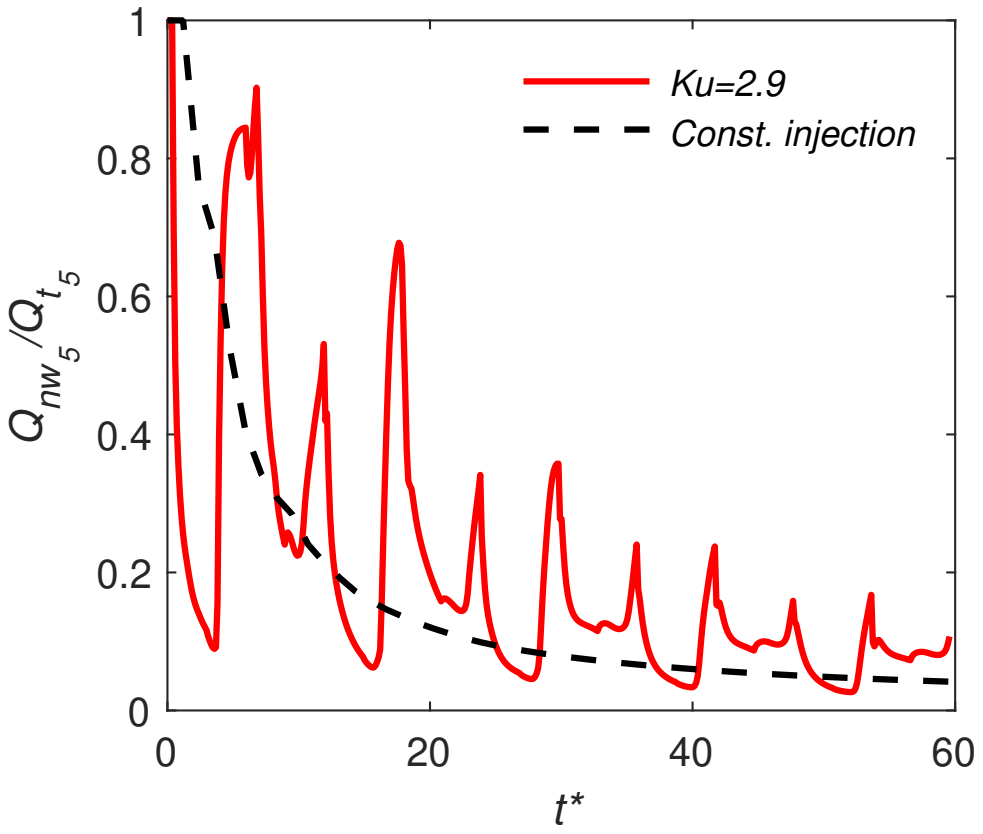

Figure 12: Comparison of temporal evolution of the NAPL flow rate recovered at the central well of the five-spot pattern produced by chaotic advection with that of the constant injection scheme obtained with the anisotropic permeability field for σ_Y^2=6 and $M = 2.2$.

4 Conclusions

We have proposed and evaluated the use of chaotic advection to enhance non-aqueous phase liquid removal during in situ soil washing remediation techniques and enhanced oil recovery in complex geological formations. Chaotic advection is generated through the application of a rotating periodic injection pulse in a five-spot injection-extraction pattern. To evaluate the method, we have performed two-phase flow simulations in multiple realizations of randomly heterogeneous permeability fields with different correlation structures and connectivity structures between injection and extraction wells. Performance metrics include removal efficiency and the distribution index of saturation (mixing). We have shown that chaotic advection can significantly improve removal efficiency and mixing. The performance of the method depends on the Kubo number, the connectivity between injection and extraction wells, the degree of heterogeneity and the mobility ratio. The most important findings are listed as follows:

1. Chaotic advection improves NAPL removal efficiency and the mixing between the wetting and non-wetting phases. This is relatively more pronounced when the permeability field displays unfavorable conditions, i.e., when the injection and extraction wells are well-connected to each other through preferential channels, the permeability field is highly heterogeneous, and/or the mobility ratio between the wetting and the

non-wetting fluid is larger than one (unfavorable displacement). This makes chaotic advection extremely useful in worst-case field applications.

2. Removal efficiency increases to a maximum value when the pulse duration of a periodically applied rotating injection pulse satisfies that the Kubo number is close to one, i.e., when the saturation front travels one range of the permeability field (an average extent of low/high permeability zones) per injection pulse. This maximum value, in an ensemble average sense, is around 12% in unfavorable conditions of the permeability field with $\sigma_Y^2 = 2$.

3. Chaotic advection can fully develop maximum strength after a few injection cycles. However, results have shown that removal efficiency should first undergo an early stage with detrimental effects in order to maximize removal in the long term.

4. The application of chaotic advection not only enhances non-aqueous phase liquid removal, but also reduces its uncertainty, making the removal system more reliable and less dependent on heterogeneity. Again, this reduction is higher in unfavorable conditions of the permeability field.

5. Maximum removal efficiency and mixing occur at different chaotic periods and removal times. In practice, the use of one or another will depend on the project objectives. For instance, at early stages of remediation one may favor removal efficiency, but at late times one may wish to promote mixing when liquid solutions with cosolvents, surfactants or polymers are meant to be used to alter fluid properties and improve performance.

6. The mobility ratio and the degree of heterogeneity are two competing factors controlling the performance of chaotic advection in two-phase flow systems. When σ_Y^2 is large the performance of chaotic advection is mainly controlled by heterogeneity. On the contrary, when σ_Y^2 is small, the mobility ratio controls the overall behavior of the system.

These results encourage the application of chaotic advection in multiphase flow problems. In this context, we note that the application of chaotic advection to NAPL polluted sites and/or enhanced oil removal comes at almost no additional cost since the removal system consisting of several wells is not necessarily modified with respect to standard practices, except for the way the technology (delivering of fluids) is put into practice. Moreover, this method can be easily implemented with other techniques to further improve removal efficiencies. The enhancement of mixing between phases can favor for instance surfactant dissolution and mobilization of NAPLs, chemical flooding or CO_2 sequestration through enhanced oil removal.

A Governing Equations in Dimensionless Form

In this appendix we show that the governing equations of the two-phase flow system can be written in a dimensionless form. The appendix shows that the Kubo number and the dimensionless variables used in our analysis arise naturally from the mass conservation equations. These quantities have therefore an important role in analyzing chaotic advection removal systems, defining the controlling parameters as well as the characteristic scales of the problem (in space and time). Let us define the following dimensionless variables,

$$x^* = \frac{x}{\ell}, \qquad y^* = \frac{y}{\ell}, \qquad t^* = \frac{v_f t}{\ell}. \tag{A.1}$$

The Darcy flux and pressure of the wetting and non-wetting fluid are written in dimensionless form as

$$q_w^* = \frac{q_w}{v_f \phi}, \qquad q_{nw}^* = \frac{q_{nw}}{v_f \phi}, \qquad p_w^* = \frac{p_w \kappa_g}{\mu_w v_f \phi \ell}, \qquad p_{nw}^* = \frac{p_{nw} \kappa_g}{\mu_w v_f \phi \ell}. \tag{A.2}$$

With these definitions, Darcy's law is expressed as

$$q_w^* = -\kappa_{rw} \exp(Y') \nabla^* p_w^*, \tag{A.3}$$

$$q_{nw}^* = -\frac{\gamma \kappa_{rnw}}{M} \exp(Y') \nabla^* p_{nw}^*, \tag{A.4}$$

where $\nabla^* = [\partial/\partial x^*, \partial/\partial y^*]$, $\gamma = \kappa_{rw}^0/\kappa_{rnw}^0$, and Y' is the deviation of the natural log of the intrinsic permeability from the mean, i.e., $Y' = Y - \langle Y \rangle$. By construction, Y' mainly depends on the degree of heterogeneity σ_Y^2, the two-point statistics (variogram), and the hydraulic connectivity CS. The injection and extraction flow rates are written in dimensionless form as

$$Q_{w_j}^{i*} = \frac{Q_{w_j}^i}{v_f \phi b \ell}, \qquad Q_{w_j}^{e*} = \frac{Q_{w_j}^e}{v_f \phi b \ell}, \qquad Q_{nw_j}^{e*} = \frac{Q_{nw_j}^e}{v_f \phi b \ell}, \qquad Q^* = \frac{Q}{v_f \phi b \ell}. \tag{A.5}$$

Substituting (A.1), (A.2) and (A.5) into (4) and (5), we have

$$\frac{\partial S_w}{\partial t^*} = -\nabla^* \cdot q_w^* + \sum_{j=1}^{n_i} Q_{w_j}^{i*}(t^*) \delta(\mathbf{x}^* - \mathbf{x}_j^{i*}) - \sum_{j=1}^{n_e} Q_{w_j}^{e*}(t^*) \delta(\mathbf{x}^* - \mathbf{x}_j^{e*}), \tag{A.6}$$

$$\frac{\partial S_{nw}}{\partial t^*} = -\nabla^* \cdot q_{nw}^* - \sum_{j=1}^{n_e} Q_{nw_j}^{e*}(t^*) \delta(\mathbf{x}^* - \mathbf{x}_j^{e*}). \tag{A.7}$$

Knowing by the properties of the Heaviside function that

$$H(t - (j-1)T/4) - H(t - jT/4) = H(t^* - (j-1)\mathrm{Ku}) - H(t^* - j\mathrm{Ku}), \tag{A.8}$$

the periodic wave function is written as

$$Q_{w_j}^{i*}(t^*) = Q^* f_j(t^*, \mathrm{Ku}), \qquad 0 \le t^* < 4\mathrm{Ku}, \tag{A.9}$$

$$Q_{w_j}^{i*}(t^*) = Q_{w_j}^{i*}(t^* - 4\mathrm{Ku}), \qquad t^* \ge 4\mathrm{Ku}, \tag{A.10}$$

where we see that the parameters controlling the governing equations can be reduced to few dimensionless parameters. The Kubo number Ku plays a central role.

Acknowledgments

This work was partially supported by the European Commission, through project MARSOLUT (grant H2020-MSCA-ITN-2018); by the Spanish Ministry of Economy and Competitiveness, through project MONOPOLIOS (RTI 2018-101990-B-100, MINECO/FEDER); and by the Catalan Agency for Management of University and Research Grants through FI 2017 (EMC/2199/2017). The MRST model and simulation data are available on Zenodo, with doi: 10.5281/zenodo.4095594.

References

Abidin, A., T. Puspasari, and W. Nugroho (2012), Polymers for Enhanced Oil Recovery Technology, *Procedia Chemistry*, doi:10.1016/j.proche.2012.06.002.

Abriola, L. M., and G. F. Pinder (1985), A Multiphase Approach to the Modeling of Porous Media Contamination by Organic Compounds: 1. Equation Development, *Water Resources Research*, doi:10.1029/WR021i001p00011.

Allen, M. B. (1985), Numerical modelling of multiphase flow in porous media, *Advances in Water Resources*, doi:10.1016/0309-1708(85)90062-4.

Amundsen, H., G. Wagner, U. Oxaal, P. Meakin, J. Feder, and T. Jøssang (1999), Slow two-phase flow in artificial fractures: Experiments and simulations, *Water Resources Research*, doi:10.1029/1999WR900147.

Arshadi, M., A. Zolfaghari, M. Piri, G. A. Al-Muntasheri, and M. Sayed (2017), The effect of deformation on two-phase flow through proppant-packed fractured shale samples: A micro-scale experimental investigation, *Advances in Water Resources*, doi:10.1016/j.advwatres.2017.04.022.

Arshadi, M., M. Khishvand, A. Aghaei, M. Piri, and G. A. Al-Muntasheri (2018), Pore-Scale Experimental Investigation of Two-Phase Flow Through Fractured Porous Media, *Water Resources Research*, doi:10.1029/2018WR022540.

Bachu, S. (2000), Sequestration of co2 in geological media: criteria and approach for site selection in response to climate change, *Energy Conversion and Management*, *41*(9), 953 – 970, doi:https://doi.org/10.1016/S0196-8904(99)00149-1.

Bagtzoglou, A. C., and P. M. Oates (2007), Chaotic advection and enhanced groundwater remediation, *Journal of Materials in Civil Engineering*, doi:10.1061/(ASCE)0899-1561(2007)19:1(75).

Bertels, S. P., D. A. DiCarlo, and M. J. Blunt (2001), Measurement of aperture distribution, capillary pressure, relative permeability, and in situ saturation in a rock fracture using computed tomography scanning, *Water Resources Research*, doi:10.1029/2000WR900316.

Bhatia, R., and C. Davis (2000), A better bound on the variance, *American Mathematical Monthly*, doi:10.2307/2589180.

Bianchi, M., C. Zheng, C. Wilson, G. R. Tick, G. Liu, and S. M. Gorelick (2011a), Spatial connectivity in a highly heterogeneous aquifer: From cores to preferential flow paths, *Water Resources Research*, *47*(5), doi:10.1029/2009WR008966.

Bianchi, M., C. Zheng, C. Wilson, G. R. Tick, G. Liu, and S. M. Gorelick (2011b), Spatial connectivity in a highly heterogeneous aquifer: From cores to preferential flow paths, *Water Resources Research*, *47*(5).

Bolster, D., M. Dentz, and J. Carrera (2009), Effective two-phase flow in heterogeneous media under temporal pressure fluctuations, *Water Resources Research*, *45*(5), doi:10.1029/2008WR007460.

Boulding, J. R. (1996), *EPA environmental assessment sourcebook*, CRC Press.

Brooks, R. H., and A. T. Corey (1966), Properties of Porous Media Affecting Fluid Flow, doi:10.3758/s13423-011-0165-y.

Brown, H. W. (1951), Capillary Pressure Investigations, *Journal of Petroleum Technology*, doi:10.2118/951067-G.

Castiglione, P. (2000), Diffusion coefficients as function of Kubo number in random fields, *Journal of Physics A: Mathematical and General*, doi:10.1088/0305-4470/33/10/302.

Celia, M. A., S. Bachu, J. M. Nordbotten, and K. W. Bandilla (2015), Status of CO2 storage in deep saline aquifers with emphasis on modeling approaches and practical simulations, doi:10.1002/2015WR017609.

Chen, Z., G. Huan, and Y. Ma (2006), *Computational methods for multiphase flows in porous media (Vol. 2)*.

Coats, K. H. (2003), IMPES stability: Selection of stable timesteps, *SPE Journal*, doi:10.2118/84924-PA.

Courant, R., K. Friedrichs, and H. Lewy (1928), On the partial difference equations of mathematical physics, *Math. Ann.*

Craig, F. F. (1971), The Reservoir Engineering Aspects of Waterflooding, in *Climate Change 2013 - The Physical Science Basis*, doi:10.1017/CBO9781107415324.004.

Craig, F. F., J. Sanderlin, D. Moore, and T. Geffen (1957), A laboratory study of gravity segregation in frontal drives, *Aime*.

Davies, R. J., S. Almond, R. S. Ward, R. B. Jackson, C. Adams, F. Worrall, L. G. Herringshaw, J. G. Gluyas, and M. A. Whitehead (2014), Oil and gas wells and their integrity: Implications for shale and unconventional resource exploitation, doi:10.1016/j.marpetgeo.2014.03.001.

De Barros, F., D. Fernàndez-Garcia, D. Bolster, and X. Sanchez-Vila (2013), A risk-based probabilistic framework to estimate the endpoint of remediation: Concentration rebound by rate-limited mass transfer, *Water Resources Research*, *49*(4), 1929–1942.

De Dreuzy, J. R., J. Carrera, M. Dentz, and T. Le Borgne (2012), Asymptotic dispersion for two-dimensional highly heterogeneous permeability fields under temporally fluctuating flow, *Water Resources Research*, *48*(1), doi:10.1029/2011WR011129.

de Marsily, G. (1985), Flow and transport in fractured rocks: connectivity and scale effect, in *International symposium on the hydrogeology of rocks of low permeability. International Association of Hydrogeologists,Tucson, AZ (USA)*, pp. 267–277.

Demond, A. H., and P. V. Roberts (1991), Effect of interfacial forces on two-phase capillary pressure—saturation relationships, *Water Resources Research*, doi:10.1029/90WR02408.

Dentz, M., and J. Carrera (2005), Effective solute transport in temporally fluctuating flow through heterogeneous media, *Water Resources Research*, *41*(8).

Di Dato, M., F. P. de Barros, A. Fiori, and A. Bellin (2018), Improving the Efficiency of 3-D Hydrogeological Mixers: Dilution Enhancement Via Coupled Engineering-Induced Transient Flows and Spatial Heterogeneity, *Water Resources Research*, doi:10.1002/2017WR022116.

Dillard, L. A., H. I. Essaid, and W. N. Herkelrath (1997), Multiphase flow modeling of a crude-oil spill site with a bimodal permeability distribution, *Water Resources Research*, doi:10.1029/97WR00857.

Dugan, P. J., J. E. McCray, and G. D. Thyne (2003), Influence of a solubility-enhancing agent (cyclodextrin) on NAPL-water partition coefficients, with implications for partitioning tracer tests, *Water Resources Research*, doi:10.1029/2002WR001672.

Edery, Y., A. Guadagnini, H. Scher, and B. Berkowitz (2014), Origins of anomalous transport in heterogeneous media: Structural and dynamic controls, *Water Resources Research*, *50*(2), 1490–1505.

Engel, J., E. Herrmann, and T. Gasser (1994), An iterative bandwidth selector for kernel estimation of densities and their derivatives, *Journal of Nonparametric Statistics*, *4*(1), 21–34, doi:10.1080/10485259408832598.

Essaid, H. I., B. A. Bekins, and I. M. Cozzarelli (2015), Organic contaminant transport and fate in the subsurface: Evolution of knowledge and understanding, *Water Resources Research*, doi:10.1002/2015WR017121.

Falta, R. W., C. M. Lee, S. E. Brame, E. Roeder, J. T. Coates, C. Wright, A. L. Wood, and C. G. Enfield (1999), Field test of high molecular weight alcohol flushing for subsurface nonaqueous phase liquid remediation, *Water Resources Research*, doi:10.1029/1999WR900097.

Fayers, F. J., and T. A. Hewett (1992), A review of current trends in petroleum reservoir description and assessment of the impacts on oil recovery, *Advances in Water Resources*, doi:10.1016/0309-1708(92)90002-J.

Fernàndez-Garcia, D., P. Trinchero, and X. Sanchez-Vila (2010), Conditional stochastic mapping of transport connectivity, *Water Resources Research*, *46*(10), doi:10.1029/2009WR008533.

Fernàndez-Garcia, D., X. Sánchez-Vila, and T. H. Illangasekare (2002), Convergent-flow tracer tests in heterogeneous media: combined experimental–numerical analysis for deter-

mination of equivalent transport parameters, *Journal of Contaminant Hydrology*, *57*(1), 129 – 145, doi:https://doi.org/10.1016/S0169-7722(01)00214-5.

Forsyth, P. A., and P. H. Sammon (1986), Practical considerations for adaptive implicit methods in reservoir simulation, *Journal of Computational Physics*, doi:10.1016/0021-9991(86)90127-0.

Glass, R. J., M. J. Nicholl, and L. Yarrington (1998), A modified invasion percolation model for low-capillary number immiscible displacements in horizontal rough-walled fractures: Influence of local in-plane curvature, *Water Resources Research*, doi:10.1029/98WR02224.

Huling, S. G., and J. W. Weaver (1991), Ground water issue: Dense non-aqueous phase liquids, *Tech. rep.*

Jackson, R. B. (2014), The integrity of oil and gas wells, doi:10.1073/pnas.1410786111.

Javanbakht, G., M. Arshadi, T. Qin, and L. Goual (2017), Micro-scale displacement of napl by surfactant and microemulsion in heterogeneous porous media, *Advances in water resources*, *105*, 173–187.

Jha, B., L. Cueto-Felgueroso, and R. Juanes (2011), Quantifying mixing in viscously unstable porous media flows, *Physical Review E - Statistical, Nonlinear, and Soft Matter Physics*, doi:10.1103/PhysRevE.84.066312.

Jin, L., S. Hawthorne, J. Sorensen, L. Pekot, B. Kurz, S. Smith, L. Heebink, V. Herdegen, N. Bosshart, J. Torres, C. Dalkhaa, K. Peterson, C. Gorecki, E. Steadman, and J. Harju (2017), Advancing CO2 enhanced oil recovery and storage in unconventional oil play—Experimental studies on Bakken shales, *Applied Energy*, doi:10.1016/j.apenergy.2017.10.054.

Journel, A., and C. Huijbregts (1976), Mining geostatistics.

Juanes, R., and K.-A. Lie (2008), Numerical modeling of multiphase first-contact miscible flows. part 2. front-tracking/streamline simulation, *Transport in porous media*, *72*(1), 97–120.

Kim, M., K. Kim, W. S. Han, J. Oh, and E. Park (2019), Density-Driven Convection in a Fractured Porous Media: Implications for Geological CO 2 Storage , *Water Resources Research*, doi:10.1029/2019wr024822.

Kitanidis, P. K. (1997), *Introduction to geostatistics: applications in hydrogeology*, Cambridge university press.

Knudby, C., and J. Carrera (2005), On the relationship between indicators of geostatistical, flow and transport connectivity, *Advances in Water Resources*, *28*(4), 405 – 421, doi:https://doi.org/10.1016/j.advwatres.2004.09.001.

Krogstad, S., K. A. Lie, O. Møyner, H. M. Nilsen, X. Raynaud, and B. Skaflestad (2015), MRST-AD - An open-source framework for rapid prototyping and evaluation of reservoir simulation problems, in *Society of Petroleum Engineers - SPE Reservoir Simulation Symposium 2015*.

Kubo, R. (1963), Stochastic Liouville equations, *Journal of Mathematical Physics*, doi:10.1063/1.1703941.

Labolle, E. M., and G. E. Fogg (2001), Role of molecular diffusion in contaminant migration and recovery in an alluvial aquifer system, in *Dispersion in Heterogeneous Geological Formations*, pp. 155–179, Springer.

Le Borgne, T., and P. Gouze (2008), Non-Fickian dispersion in porous media: 2. Model validation from measurements at different scales, *Water Resources Research*, doi:10.1029/2007WR006279.

Le Borgne, T., M. Dentz, D. Bolster, J. Carrera, J.-R. De Dreuzy, and P. Davy (2010), Non-fickian mixing: Temporal evolution of the scalar dissipation rate in heterogeneous porous media, *Advances in Water Resources*, *33*(12), 1468–1475.

Lester, D., G. Metcalfe, M. Trefry, A. Ord, B. Hobbs, and M. Rudman (2009), Lagrangian topology of a periodically reoriented potential flow: Symmetry, optimization, and mixing, *Physical Review E*, *80*(3), 036,208.

Lester, D., M. Rudman, G. Metcalfe, M. Trefry, A. Ord, and B. Hobbs (2010), Scalar dispersion in a periodically reoriented potential flow: Acceleration via lagrangian chaos, *Physical Review E*, *81*(4), 046,319.

Lester, D. R., G. Metcalfe, and M. G. Trefry (2013), Is chaotic advection inherent to porous media flow?, *Physical Review Letters*, doi:10.1103/PhysRevLett.111.174101.

Leverett, M. (1939), Flow of Oil-water Mixtures through Unconsolidated Sands, *Petroleum Transactions of AIME*, doi:10.2118/939149-g.

Leverett, M. (1941), Capillary Behavior in Porous Solids, *Transactions of the AIME*, doi:10.2118/941152-G.

Libera, A., F. P. de Barros, and A. Guadagnini (2017), Influence of pumping operational schedule on solute concentrations at a well in randomly heterogeneous aquifers, *Journal of Hydrology*, doi:10.1016/j.jhydrol.2016.12.022.

Lie, K. (2014), An introduction to reservoir simulation using MATLAB: user guide for the Matlab Reservoir Simulation Toolbox (MRST), *SINTEF ICT*.

Luo, J., M. Dentz, J. Carrera, and P. Kitanidis (2008), Effective reaction parameters for mixing controlled reactions in heterogeneous media, *Water Resources Research*, doi:10.1029/2006WR005658.

Mackay, D. M., and J. A. Cherry (1989), Groundwater contamination: pump-and-treat remediation, *Environmental Science & Technology*, *23*(6), 630–636, doi:10.1021/es00064a001.

Martel, R., A. Hébert, R. Lefebvre, P. Gélinas, and U. Gabriel (2004), Displacement and sweep efficiencies in a dnapl recovery test using micellar and polymer solutions injected in a five-spot pattern, *Journal of Contaminant Hydrology*, *75*(1), 1 – 29, doi:https://doi.org/10.1016/j.jconhyd.2004.03.007.

Mays, D. C., and R. M. Neupauer (2012), Plume spreading in groundwater by stretching and folding, *Water Resources Research*, doi:10.1029/2011WR011567.

Mazzino, A. (1997), Effective correlation times in turbulent scalar transport, *Physical Review E - Statistical Physics, Plasmas, Fluids, and Related Interdisciplinary Topics*, doi:10.1103/PhysRevE.56.5500.

Mccray, J. E., and M. L. Brusseau (1999), Cyclodextrin-enhanced in situ flushing of multiple-component immiscible organic liquid contamination at the field scale: Analysis of dissolution behavior, *Environmental Science and Technology*, doi:10.1021/es980117b.

Metcalfe, G., M. Rudman, A. Brydon, L. Graham, and R. Hamilton (2006), Composing chaos: An experimental and numerical study of an open duct mixing flow, *AIChE Journal*, *52*(1), 9–28.

Metcalfe, G., D. Lester, A. Ord, P. Kulkarni, M. Rudman, M. Trefry, B. Hobbs, K. Regenaur-Lieb, and J. Morris (2010), An experimental and theoretical study of the mixing characteristics of a periodically reoriented irrotational flow, *Philosophical Transactions of the Royal Society A: Mathematical, Physical and Engineering Sciences*, *368*(1918), 2147–2162.

Neupauer, R. M., J. D. Meiss, and D. C. Mays (2014), Chaotic advection and reaction during engineered injection and extraction in heterogeneous porous media, *Water Resources Research*, doi:10.1002/2013WR014057.

Nicolaides, C., B. Jha, L. Cueto-Felgueroso, and R. Juanes (2015), Impact of viscous fingering and permeability heterogeneity on fluid mixing in porous media, *Water Resources Research*, doi:10.1002/2014WR015811.

NRC (2005), *Contaminants in the Subsurface: Source Zone Assessment and Remediation*, Washington, DC: The National Academies Press., doi:10.17226/11146.

Ottino, J. (1990), Mixing, Chaotic Advection, And Turbulence, *Annual Review of Fluid Mechanics*, doi:10.1146/annurev.fluid.22.1.207.

Ottino, J. M., S. C. Jana, and V. S. Chakravarthy (1994), From Reynolds's stretching and folding to mixing studies using horseshoe maps, *Physics of Fluids*, doi:10.1063/1.868309.

Paez Yanez, P. A., J. L. Mustoni, H. Frampton, M. F. Relling, K.-T. Chang, and P. C. Hopkinson (2007), New Attempt in Improving Sweep Efficiency at the Mature Koluel Kaike and Piedra Clavada Waterflooding Projects of the S. Jorge Basin in Argentina, doi:10.2118/107923-MS.

Piscopo, A. N., R. M. Neupauer, and D. C. Mays (2013), Engineered injection and extraction to enhance reaction for improved in situ remediation, *Water Resources Research*, doi:10.1002/wrcr.20209.

Pruess, K., and Y. W. Tsang (1990), On two-phase relative permeability and capillary pressure of rough-walled rock fractures, *Water Resources Research*, doi:10.1029/WR026i009p01915.

Raffa, P., A. A. Broekhuis, and F. Picchioni (2016), Polymeric surfactants for enhanced oil recovery: A review, doi:10.1016/j.petrol.2016.07.007.

Rangel-German, E. R., and A. R. Kovscek (2006), A micromodel investigation of two-phase matrix-fracture transfer mechanisms, *Water Resources Research*, doi:10.1029/2004WR003918.

Rao, P. S. C., M. D. Annable, R. K. Sillan, D. Dai, K. Hatfield, W. D. Graham, A. L. Wood, and C. G. Enfield (1997), Field-scale evaluation of in situ cosolvent flushing for enhanced aquifer remediation, *Water resources research*, *33*(12), 2673–2686.

Reid, R. C., J. M. Prausnitz, and T. K. Sherwood (1997), *The properties of gases and liquids*, 4th ed. ed., McGraw-Hill,New York.

Ren, B., and I. Duncan (2019), Modeling oil saturation evolution in residual oil zones: Implications for CO2 EOR and sequestration, *Journal of Petroleum Science and Engineering*, doi:10.1016/j.petrol.2019.02.072.

Renard, P., and D. Allard (2013a), Connectivity metrics for subsurface flow and transport, *Advances in Water Resources*, *51*, 168 – 196, doi:https://doi.org/10.1016/j.advwatres.2011.12.001, 35th Year Anniversary Issue.

Renard, P., and D. Allard (2013b), Connectivity metrics for subsurface flow and transport, *Advances in Water Resources*, *51*, 168–196.

Rodríguez-Escales, P., D. Fernàndez-Garcia, J. Drechsel, A. Folch, and X. Sanchez-Vila (2017), Improving degradation of emerging organic compounds by applying chaotic advection in Managed Aquifer Recharge in randomly heterogeneous porous media, *Water Resources Research*, doi:10.1002/2016WR020333.

Saaltink, M. W., V. Vilarrasa, F. De Gaspari, O. Silva, J. Carrera, and T. S. Rötting (2013), A method for incorporating equilibrium chemical reactions into multiphase flow models for co2 storage, *Advances in Water Resources*, *62*, 431 – 441, doi:https://doi.org/10.1016/j.advwatres.2013.09.013, computational Methods in Geologic CO2 Sequestration.

Sammon, P. H. (1988), Analysis of upstream differencing, *SPE Reservoir Engineering (Society of Petroleum Engineers)*, doi:10.2118/14045-PA.

Satkin, R. L., and P. B. Bedient (1988), Effectiveness of various aquifer restoration schemes under variable hydrogeologic conditions, *Groundwater*, *26*(4), 488–498.

Schwille, F. (1981), Groundwater pollution in porous media by fluids immiscible with water, in *Studies in Environmental Science*, doi:10.1016/S0166-1116(08)71937-X.

Silliman, S., and A. Wright (1988), Stochastic analysis of paths of high hydraulic conductivity in porous media, *Water Resources Research*, *24*(11), 1901–1910.

Sleep, B. E., and J. F. Sykes (1989), Modeling the transport of volatile organics in variably saturated media, *Water Resources Research*, doi:10.1029/WR025i001p00081.

Sleep, B. E., and J. F. Sykes (1993a), Compositional simulation of groundwater contamination by organic compounds: 1. Model development and verification, *Water Resources Research*, doi:10.1029/93WR00283.

Sleep, B. E., and J. F. Sykes (1993b), Compositional simulation of groundwater contamination by organic compounds: 2. Model applications, *Water Resources Research*, doi:10.1029/93WR00284.

Smalley, P., A. Ross, C. Brown, T. Moulds, and M. Smith (2009), Reservoir Technical Limits: A Framework for Maximizing Recovery From Oil Fields, *SPE Reservoir Evaluation & Engineering*, doi:10.2118/109555-PA.

Soga, K., J. Page, and T. Illangasekare (2004), A review of napl source zone remediation efficiency and the mass flux approach, *Journal of Hazardous Materials*, *110*(1), 13 – 27, doi:https://doi.org/10.1016/j.jhazmat.2004.02.034.

Stroo, H. F., A. Leeson, J. A. Marqusee, P. C. Johnson, C. H. Ward, M. C. Kavanaugh, T. C. Sale, C. J. Newell, K. D. Pennell, C. A. Lebrón, and M. Unger (2012), Chlorinated ethene source remediation: Lessons learned, *Environmental Science & Technology*, *46*(12), 6438–6447, doi:10.1021/es204714w, pMID: 22558915.

Sánchez-Vila, X., P. M. Meier, and J. Carrera (1999), Pumping tests in heterogeneous aquifers: An analytical study of what can be obtained from their interpretation using jacob's method, *Water Resources Research*, *35*(4), 943–952, doi:10.1029/1999WR900007.

Trefry, M. G., D. R. Lester, G. Metcalfe, A. Ord, and K. Regenauer-Lieb (2012a), Toward enhanced subsurface intervention methods using chaotic advection, *Journal of Contaminant Hydrology*, *127*(1), 15 – 29, doi:https://doi.org/10.1016/j.jconhyd.2011.04.006, gQ10: Groundwater Quality Management in a Rapidly Changing World.

Trefry, M. G., D. R. Lester, G. Metcalfe, A. Ord, and K. Regenauer-Lieb (2012b), Toward enhanced subsurface intervention methods using chaotic advection, *Journal of Contaminant Hydrology*, *127*(1-4), 15–29.

Trinchero, P., X. Sánchez-Vila, and D. Fernàndez-Garcia (2008), Point-to-point connectivity, an abstract concept or a key issue for risk assessment studies?, *Advances in Water Resources*, *31*(12), 1742 – 1753, doi:https://doi.org/10.1016/j.advwatres.2008.09.001.

Vilarrasa, V., D. Bolster, S. Olivella, and J. Carrera (2010), Coupled hydromechanical modeling of co2 sequestration in deep saline aquifers, *International Journal of Greenhouse Gas Control*, *4*(6), 910 – 919, doi:https://doi.org/10.1016/j.ijggc.2010.06.006, cO2 Storage at the EGU General Assembly 2009.

Vlad, M., F. Spineanu, J. Misguich, and R. Balescu (2001), Diffusion in biased turbulence, *Physical Review E*, *63*(6), 066,304.

Wan, J., T. K. Tokunaga, C. F. Tsang, and G. S. Bodvarsson (1996), Improved glass micromodel methods for studies of flow and transport in fractured porous media, *Water Resources Research*, doi:10.1029/96WR00755.

Welkenhuysen, K., J. Rupert, T. Compernolle, A. Ramirez, R. Swennen, and K. Piessens (2017), Considering economic and geological uncertainty in the simulation of realistic investment decisions for CO2-EOR projects in the North Sea, *Applied Energy*, doi:10.1016/j.apenergy.2016.10.105.

Western, A. W., G. Blöschl, and R. B. Grayson (2001), Toward capturing hydrologically significant connectivity in spatial patterns, *Water Resources Research*, *37*(1), 83–97, doi:10.1029/2000WR900241.

Wipfler, E. L., M. I. Van Dijke, and S. E. Van Der Zee (2004), Three-phase flow analysis of dense nonaqueous phase liquid infiltration in horizontally layered porous media, *Water Resources Research*, doi:10.1029/2003WR002948.

Wu, Y. P. S. Huyakorn, and N. S. Park (1994), A vertical equilibrium model for assessing nonaqueous phase liquid contamination and remediation of groundwater systems, *Water Resources Research*, doi:10.1029/93WR03412.

Yanosik, J., and T. McCracken (1979), A Nine-Point, Finite-Difference Reservoir Simulator for Realistic Prediction of Adverse Mobility Ratio Displacements, *Society of Petroleum Engineers Journal*, doi:10.2118/5734-PA.

Yousefvand, H., and A. Jafari (2015), Enhanced oil recovery using polymer/nanosilica, *Procedia Materials Science*, *11*, 565 – 570, doi:https://doi.org/10.1016/j.mspro.2015.11.068, 5th International Biennial Conference on Ultrafine Grained and Nanostructured Materials, UFGNSM15.

Zhang, P., S. L. Devries, A. Dathe, and A. C. Bagtzoglou (2009), Enhanced mixing and plume containment in porous media under time-dependent oscillatory flow, *Environmental Science and Technology*, doi:10.1021/es900854r.

Zheng, C., and S. M. Gorelick (2003), Analysis of solute transport in flow fields influenced by preferential flowpaths at the decimeter scale, *Groundwater*, *41*(2), 142–155, doi:10.1111/j.1745-6584.2003.tb02578.x.

Zhong, L., A. Mayer, and R. J. Glass (2001), Visualization of surfactant-enhanced nonaqueous phase liquid mobilization and solubilization in a two-dimensional micromodel, *Water*

Resources Research, doi:10.1029/2000WR900300.